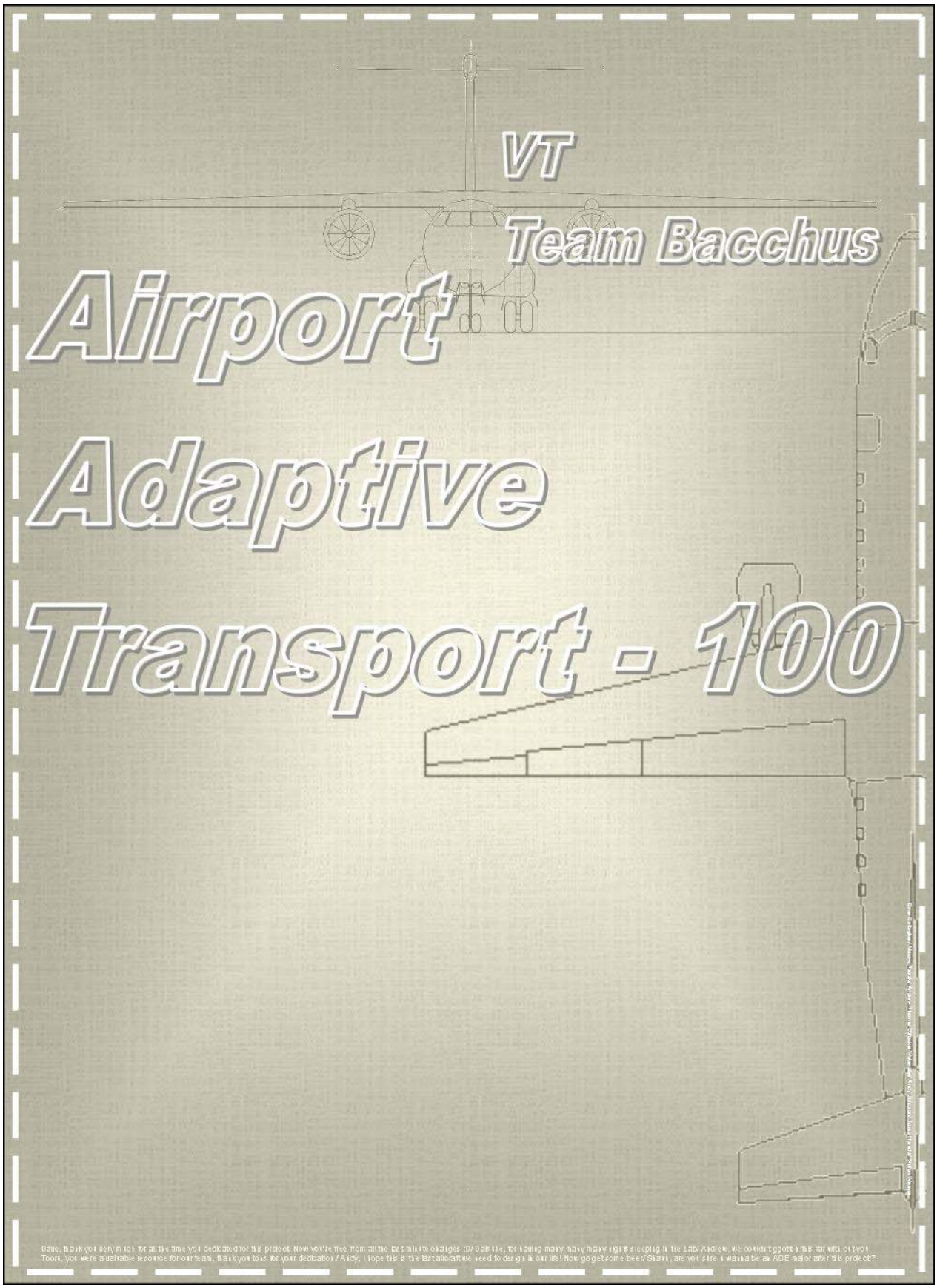

Dave, thank you very much for all the time you dedicated for this project. Now you're free from all the last-minute changes :D / Bakke, for having many many many sigils sleeping in the Lab / Andrew, we couldn't go this far with out you. Toon, you were a valuable resource for our team, thank you too! for your dedication / Andy, I hope this is the last aircraft we need to design in our life! Now go get some beer! Shawn, are you sure it was a be an ACE major after this project?

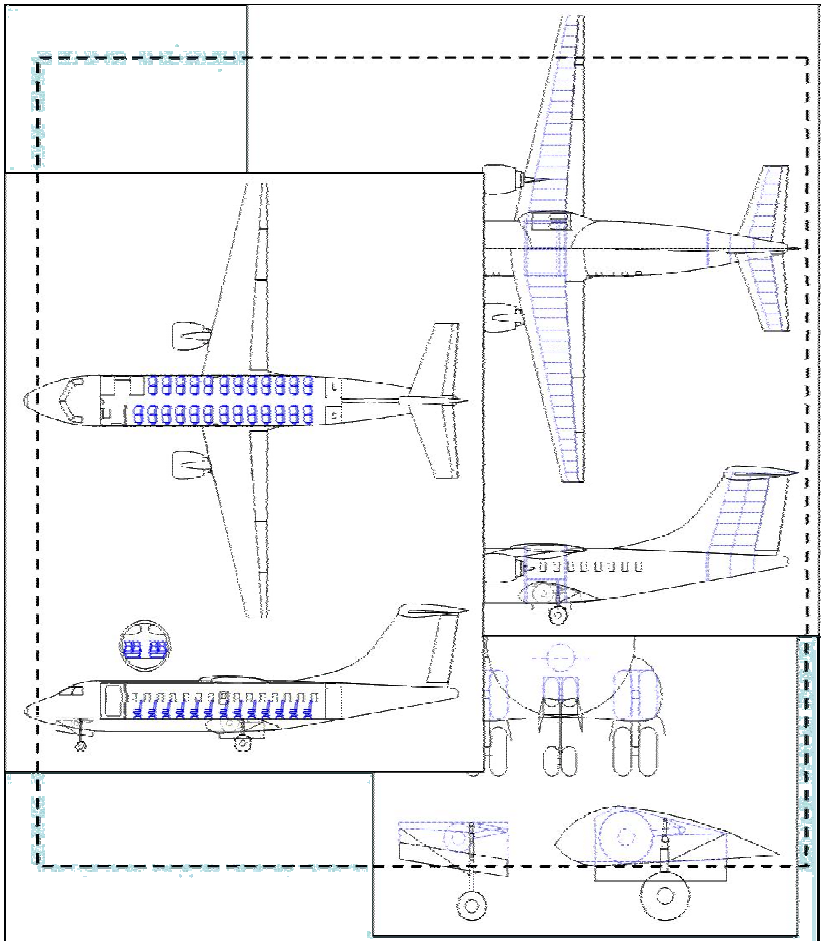

David Gallagher			
	Student Signature	Date	AIAA Number
Masaki Tasaki			
	Student Signature	Date	AIAA Number
Daisuke Watanabe			
	Student Signature	Date	AIAA Number
Andrew Johnson			
	Student Signature	Date	AIAA Number
Tooru Harada			
	Student Signature	Date	AIAA Number
Andrew Thorne			
	Student Signature	Date	AIAA Number
Dr. W.H. Mason			
	Signature	Date	AIAA Number

Team Bacchus is proud to present the answer to overcrowding at major airports, the Airport Adaptive Transport (AAT). The AAT, not only carries 50 passengers a block range of 1500 nm, but also has the capability of utilizing hundreds of short field airports by employing high lift devices to takeoff and land on runways of only 2500 ft. Aside from the benefits of increased passenger service, the AAT can be equipped to serve in the Civil Reserve Fleet. In this instance, the AAT can be outfitted in a variety of different interior configurations. This allows for the AAT to act as a wildfire support aircraft and a troop transport, although further modifications may be possible depending on the buyer's request. All these benefits, and the AAT still cost roughly the same as a conventional regional jet (RJ). While the details of the design are described in the report, the basic geometry is illustrated in the figure shown below and a more detailed illustration is located on the foldout on the next page.

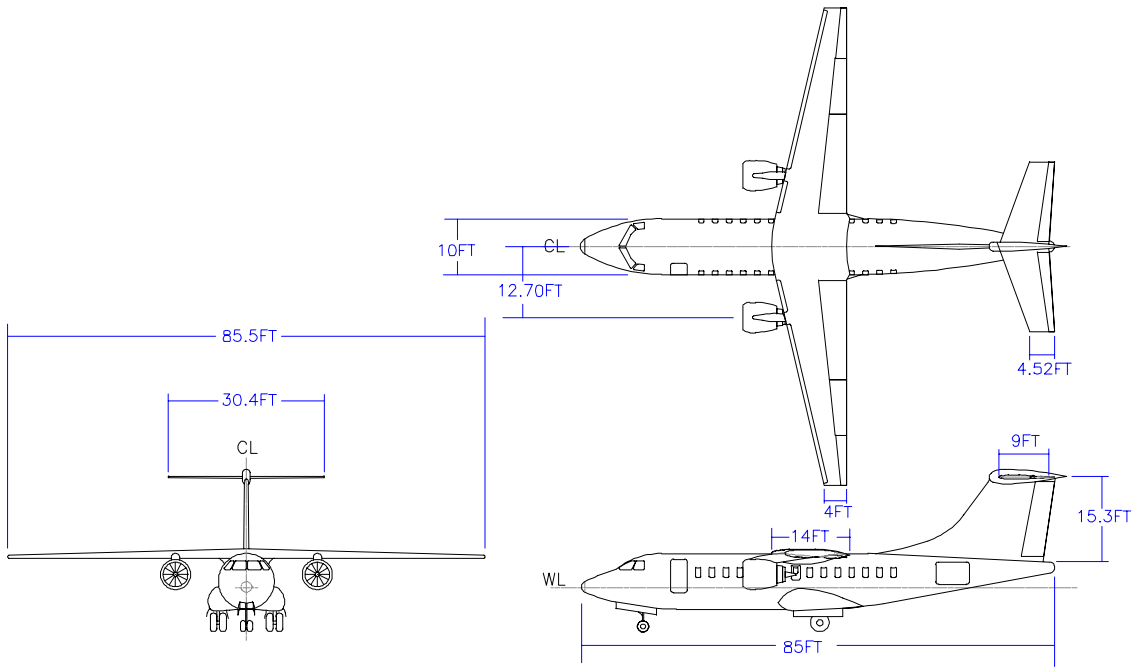

AAT-100 DATA

50 PASSENGER STOL REGIONAL JET

FUSELARGE LENGTH = 85 FT
FUSELAGE WIDTH = 10 FT

PRIMARY
EMPTY WEIGHT = 31,405 LBS
TOGW = 53,557 LBS
SECONDARY
EMPTY WEIGHT = 29,720 LBS
TOGW = 48,782 LBS

ENGINES: GE 34-8C1 TURBOFAN ENGINE x2
MAX THRUST (@SL) = 12,670 LBS x2
BYPASS RATIO = 5
SFC AT TAKE OFF = 0.37 - 0.39

CRUISE SPEED = 400 KNOTS
STALL SPEED = 50 KNOTS

AIRFOIL DATA	WING	HOR. TAIL	VERT. TAIL
AIRFOIL DESIGNATION	NASA SC(2)-0712	NACA 0008	NACA 0012
SPAN (FT)	85.5	30.4	15.3
REF. AREA (FT^2)	769.5	205.72	235.3
AR	9.5	4.5	1.0
CR (FT)	14.0	9.0	17.0
CT (FT)	4.0	4.52	13.68
MAC (FT)	9.926	7.01	15.35
LE SWEEP (DEG.)	13.0	20.0	20.0
HIGH LIFT DEVICE: EXTERNAL BLOWN FLAPS			

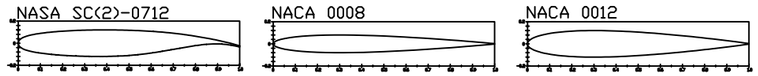

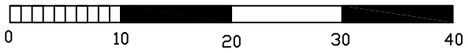

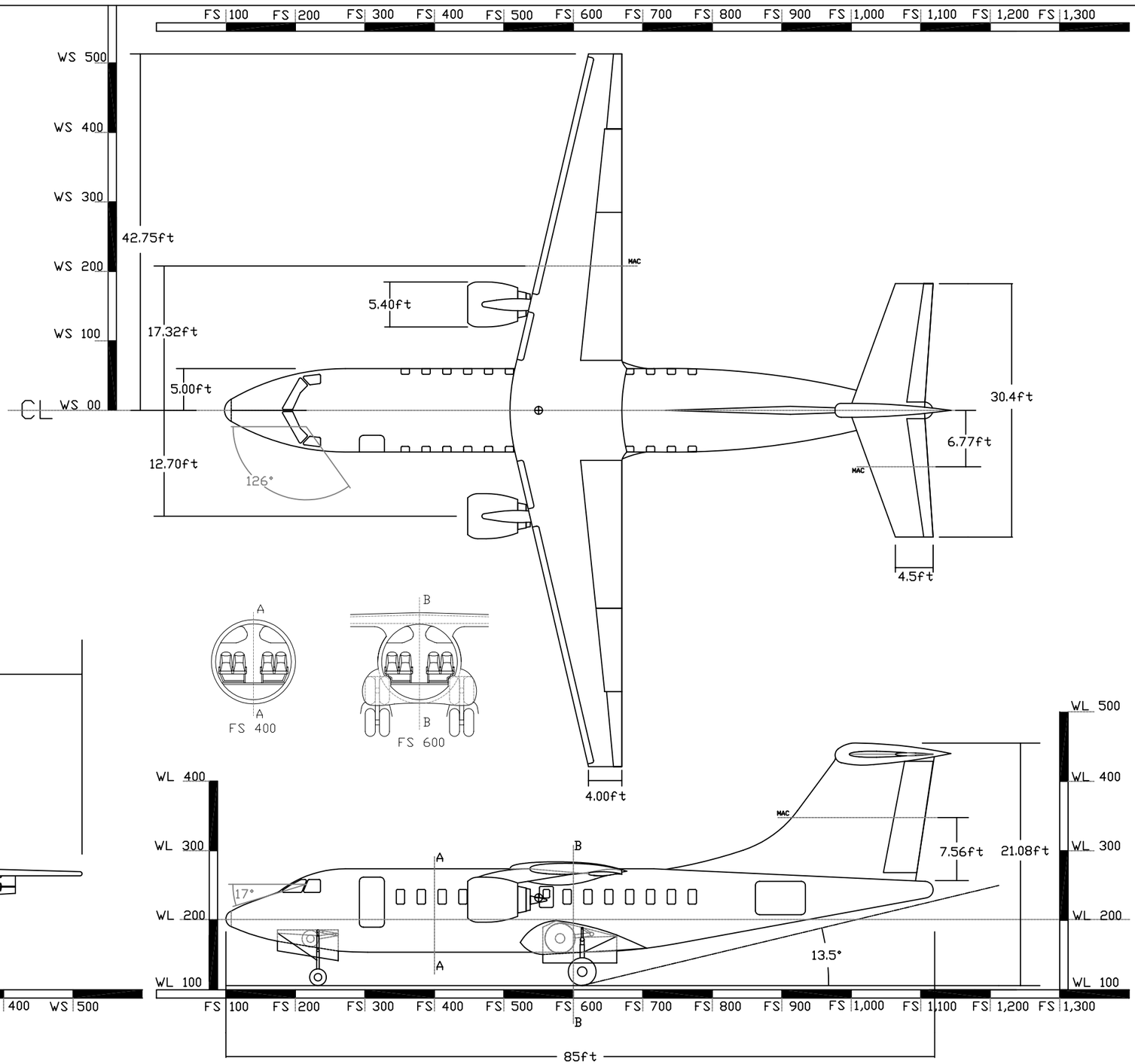

TEAM BACCHUS	
GENERAL ARRANGEMENT	AIRCRAFT MODEL: AAT-100
	DRAWING VERSION: 5.6
	REVISION DATE: 5/6/2004 M.T.

Table Of Contents

Table Of Figures

Table Of Tables

Abbreviations

AAT	Airport Adaptive Transport
STOL	Short TakeOff and Landing
RJ	Regional Jet
AIAA	American Institute of Aeronautics and Astronautics
RFP	Request For Proposal
SNI	Simultaneous Non-Interfering
BFL	Balanced Field Length
FAR	Federal Aviation Regulations
IMC	Instrument Meteorological Conditions
USB	Upper Surface Blowing
FOD	Foreign Object Damage
EBF	Externally Blown Flaps
FOM	Figure Of Merits
TOGW	TakeOff Gross Weight
CG	Center of Gravity
MAC	Mean Aerodynamic Chord
SFC	Specific Fuel Consumption
LE	Leading Edge
NASA	National Aeronautics and Space Administration
NACA	National Advisory Committee on Aeronautics
QSRA	Quiet Short haul Research Aircraft
IBF	Internally Blown Flaps
HUD	Heads-Up Display
MFD	Multi-Function Display
FCS	Flight Control System
SCAS	Stability and Control Augmentation System
TMS	Thrust Management System
EFDS	Engine Failure Detection System
APU	Auxiliary Power Unit
RDT&E	Research /Development and Testing and Evaluation
OC	Operating Cost
IOC	Indirect Operational Cost
DOC	Direct Operating Cost

Variables

v_{tas}	True Airspeed
C_{LMax}	Maximum Three Dimensional Lift Coefficient
C_D	Coefficient of Drag
$TOGW$	Takeoff Gross Weight
T/W	Thrust-to-Weight Ratio
W/S	Wing Loading
C_L	Three Dimensional Lift Coefficient
SFC	Specific Fuel Consumption
S	Area
AR	Aspect Ratio
c_r	Root Chord
c_t	Tip Chord
c_{bar}	Average Chord
b	Span
l	Taper Ratio
M_{DD}	Drag Divergent Mach Number
C_l	Two Dimensional Lift Coefficient
t/c	Thickness-to-Chord Ratio
K_a	Airfoil Technology Factor
L	Sweep
DC_L	Three Dimensional Lift Coefficient Increment
C_m	Jet Momentum Coefficient
w_j	Weight Rate Of Jet Flow
V_j	Jet Velocity
g	Acceleration Due To Gravity
q	Dynamic Pressure
$(C_L)_{Cm = 0}$	Lift Coefficient When The Blowing Coefficient Is Zero
d_j	Deflection Angle Of The Jet Exhaust
a	Angle Of Attack
$C_{L,G}$	Jet-Circulation Lift Coefficient
x	Distance From Aircraft's Nose (Positive In Aft Direction)
y	Distance From Aircraft's Centerline (Positive In Starboard Direction)
S_H	Area Of The Horizontal Tail Surface

V_H	Horizontal Tail Volume
S_W	Wing Area
c_{barW}	Average Chord Of The Wing
l_H	Horizontal Moment Arm
S_V	Area Of The Vertical Tail Surface
V_V	Vertical Tail Volume
l_V	Vertical Moment Arm
C_{Lda}	Change In Lift Coefficient Due To An Aileron Deflection
C_{Mda}	Change In Moment Coefficient Due To An Aileron Deflection
C_{L0}	Lift Coefficient When Angle of Attack Is Zero
C_{M0}	Moment Coefficient When Angle Of Attack Is Zero
C_M	Moment Coefficient
V_B	Stall Boundary Velocity
V_C	Cruise Velocity
V_D	Dive Velocity
C_{MAN}	Manufacturing Cost
C_{ACQ}	Acquisition Cost
C_{OPS}	Operating Cost
C_{DISP}	Disposal Cost
LCC	Life Cycle Cost
AEP	Airplane Estimated Price
PM	Primary Mission
SM	Secondary Mission

I. Introduction:

In recent years, our nation's airports have seen a substantial strain due to the increase in the numbers of aircraft operations. Since 9/11, airport traffic has decreased slightly, but congestion is still a problem. One approach to alleviating this problem is to develop aircraft that takeoff and land on runways of 2500 ft, approximately half that of comparator commercial aircraft, with the provision that said aircraft would cruise at similar altitudes, speeds, and efficiencies of existing aircraft. This criterion would allow for an aircraft to operate on a runway that is not normally utilized for commercial air travel, thus allowing for two aircraft to land in a time slot where only one could land before. Another possibility would be for the aircraft to be diverted away from a major airport to a smaller landing field thus allowing for commuters to land at an airport that is closer to their final destination. Team Bacchus is pleased to provide such a solution to this critical transportation issue.

The objective of this project was to design an aircraft that applies short takeoff and landing (STOL) technologies to a series of aircraft. The aircraft will be available in two different configurations that the buyer must choose from initially. The first configuration will allow for commercial use only as an RJ, and the other will have the option of serving in the Civil Reserve Fleet as a wildfire support vehicle. The secondary aircraft configuration will have an incremental cost associated with it due to increased technological demands and outfitting that the government will partially subsidize with the understanding that they can call the aircraft into service at any time.

II. Request For Proposal (RFP):

The requirements set forth by the American Institute of Aeronautics and Astronautics (AIAA) Foundation call for an "airport adaptive regional transport with a secondary role to support homeland security" (Ref. 1).

1. Design Objective

With more people traveling more often than ever before, the effect of overcrowding in the air can create a "traffic jam" at major airports. The easiest way to alleviate some of the overcrowding, and to cut down on some of the associated time delays of aircraft sitting either in a holding pattern or waiting to takeoff, is to divert some of the flights to other airports. However, since most aircraft require the longer runways of the larger airports, this is not a feasible solution. The AAT alleviates this problem. The AAT is designed with STOL technologies in mind, thereby allowing it to use shorter runways. The other problem that arises is in the overlapping of approach patterns. The AAT is specifically required to conduct simultaneous non-interfering (SNI) landings, consisting of a decelerating, constant radius spiral, which will allow it to slow down from conventional approach speeds of 140-170 kts to a STOL landing speed of around 65 kts. This type of landing pattern allows for either the simultaneous landing of multiple aircraft with different trajectories at large airports, or the diversion of the AAT to a smaller airfield.

Events that have taken place in recent years demonstrate the severity of unsupported acts of terrorism and the need to move supplies and troops effectively and quickly in the event of an attack. Also, in response to the growing number of wildfires in

the western sections of the United States, and the outward expansion of the population into these fire-prone regions, the need has arisen for a transport that can quickly move firefighters, their equipment, and other emergency personal to areas in need.

There are three main objectives for the aircraft to be competitive in the world market. First, it will need to be cost effective and efficient, in order to give the airline industry the best aircraft for their money. Second, it will need to have the ability to conduct STOL takeoffs and landings utilizing the SNI approach, to alleviate some of the wait time for the passengers and airlines. Third, it must be able to accommodate the various secondary missions, such that it can better serve both the people and the government. The design that does this will have the best qualifications and will prove to be the most marketable. Team Bacchus has provided just such a design in the following report.

2. Mission Summary

The regional transport is required by the AIAA to be a 49 passenger RJ with a balanced field length (BFL) of 2500 ft. It is required to cruise at a minimum velocity of 400 kts and to have a block range of 1500 nm with FAR 25 reserves. Aside from a shorter than average takeoff length, the aircraft must be able to conduct a SNI adverse weather approach to a large airport, and land on runways that are not normally used by commercial aircraft. The landing process must be a spiral landing consisting of as many circular loops as it takes to reach the ground by using reasonable turning and deceleration rates. This must be able to be completed with one engine inoperative in IMC (Cat 3C)

conditions. This aircraft must be designed to be more affordable and more efficient than existing aircraft.

The secondary mission to be performed is for this aircraft to serve in the Civil Reserve Fleet such that, in a time of crisis, the government would use the aircraft to transport firefighters and other emergency personnel. In this role, the aircraft would have its passenger accommodations removed and a mission specific set of accommodations installed temporarily. The secondary mission to be performed must include one in which the aircraft transports people and equipment to a remote area with a shorter than average runway. There are a variety of other suggested missions, including, but not limited to, an emergency response vehicle or air ambulance. For any of these missions, the aircraft is required to hold half its normal payload, cruise 750 nm onto semi-prepared runways of not less than 1000 ft, and return to the initial base.

To make this multi-mission aircraft more appealing to the aircraft industry, separate flyaway costs must be calculated for the aircraft's primary and secondary mission, for which the government will subsidize the difference with the understanding that it can call the aircraft into service at any time.

Along with secondary missions, the aircraft must be able to be upgraded in the conventional sense through the use of fuselage plugs. These plugs would be used to create two additional models that would hold 65 and 81 passengers.

A summary of both missions is shown on the next page in Table II.1.

Table II.1: Mission Summary

	Units	Primary Mission	Secondary Mission
Passengers	--	49	20
Crew	--	3	3
Passenger Weight	lbs	185	165
Baggage Weight	lbs	45	144
Additional Weight	lbs	--	2000
BFL	ft	2500	2000
Cruise Speed	kts	400	400
Block Range	nm	1500	1500 (2 X 750)
Reserves	--	FAR 25	--
Landing Type	--	SNI in IMC (Cat 3C)	--
Diversion	nm	150	--
Holding	min	45	--

3. Details And Requirements

The mission segments with the power settings and the times allotted are given in Figure II.1 and in Figure II.2.

3.1 Primary Mission Details

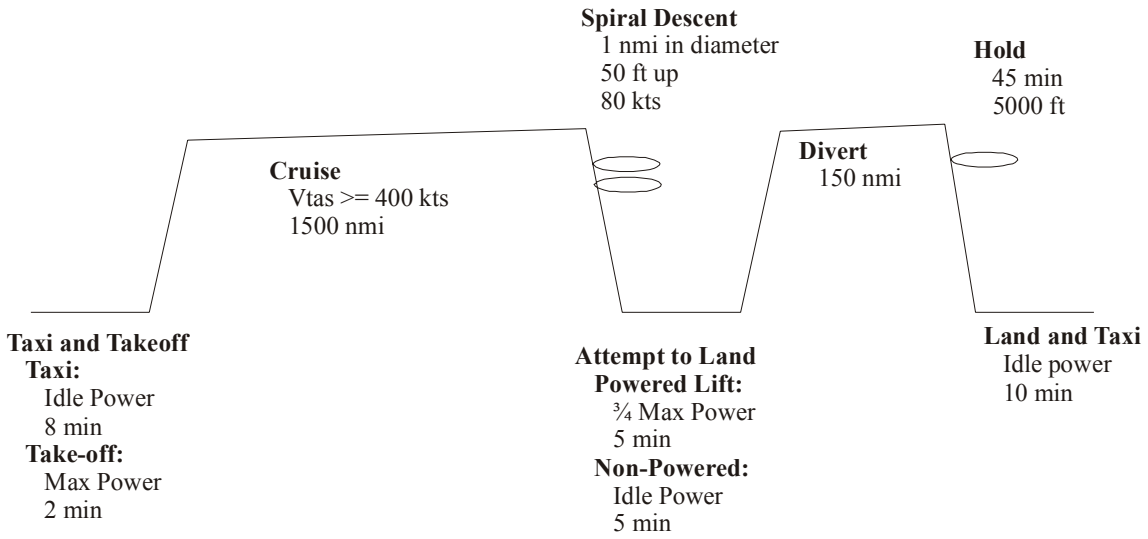

Figure II.1: Primary Mission Diagram

Accompanying the above mission diagram, Figure II.1, more specific requirements that focused on the descent were specified. The aircraft must be able to

follow a Jonez Four STAR approach into Dallas Ft. Worth International. Upon entering the SNI landing, the nominal sink rate is 15 ft/sec. The aircraft must be able to execute a fully automated SNI landing with one engine out.

3.2 Wildfire Support Mission Details

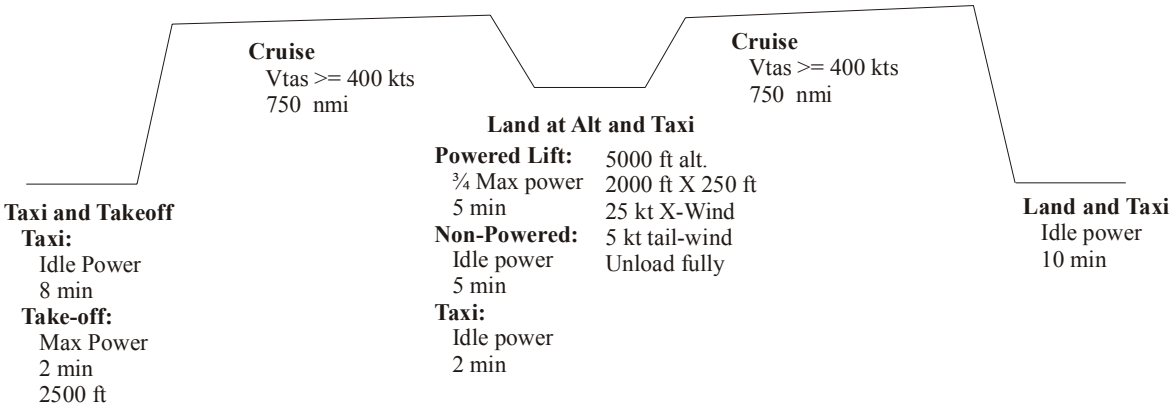

Figure II.2: Wildfire Support Mission Diagram

Accompanying the above mission diagram, Figure II.2, other requirements were specified. The runway at altitude has 50 ft high obstacles at either end and is oriented in a less-than-optimal direction. One thing to note is that neither the SNI landing, nor the diversion specified for the primary mission is required for this mission.

III. Project Drivers:

A number of parameters were set forth in the RFP's description of the primary mission; however only two are project drivers. One of the key requirements in the RFP is that the AAT has a balanced field length of only 2500 ft. This is significantly shorter than that of comparator aircraft. The CRJ-200, which is roughly the same size as the AAT, needs a BFL of 5800 ft at maximum takeoff weight. This means that the AAT will be a STOL vehicle, requiring some type of device to achieve a higher lift coefficient (C_L). This can be done in a variety of ways, such as mechanical flap deployment, vectored thrust, or powered lift. After doing preliminary calculations, it was found that the maximum lift coefficient (C_{LMax}) required is dictated by the landing field length and was found to be 6.5. In contrast, C_{LMax} for takeoff is 5.8.

The next project driver to be considered is the automated SNI landing. The SNI landing can be visualized in Figure III.1, which was created using the AIAA provided trajectories.

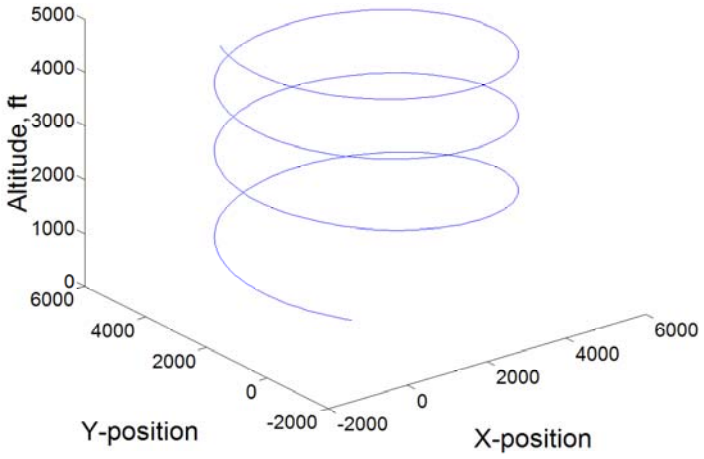

Figure III.1: AIAA Supplied SNI Landing Trajectories

This particular pattern requires both banking and deceleration, meaning that the load factor has the capability of becoming higher than normal. From the AIAA provided data, a plot of the load factor versus the time (Figure III.2) was made taking into account both vertical and horizontal deceleration along with the banking of the aircraft.

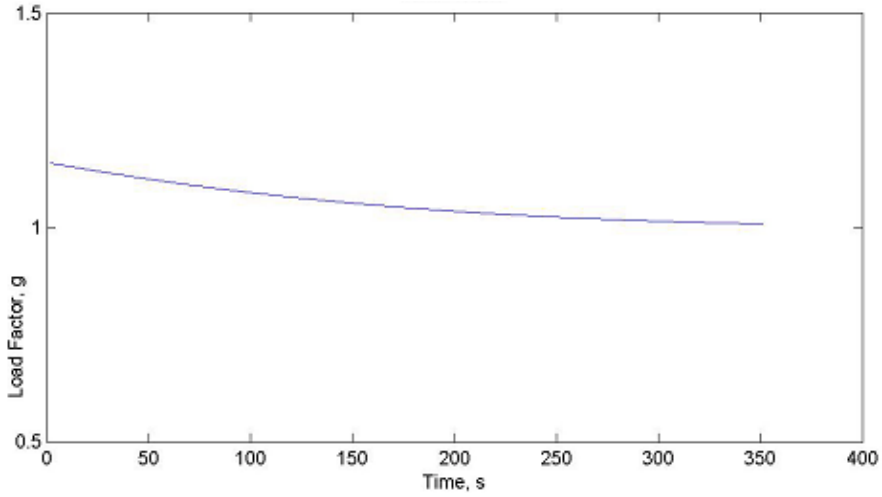

Figure III.2: AIAA Supplied Load Factor

From Figure III.2 we can see that the maximum load factor incurred is only 1.15, which is acceptable for a commercial transport.

The RFP's description for the wildfire mission specifies one main project driver; the AAT will have to be able to land on a semi-prepared runway with a BFL of 2000 ft.

IV. Initial Concepts And Descriptions:

To respond to the RFP, each group member contributed a conceptual aircraft design. After examining the six concepts, we quickly decided that some shared many features, which allowed us to combine them and narrow the field down to three concepts. Those three concepts and the method of final selection are presented in the following sections.

1. Design One

Design One, illustrated in Figure IV.1, has a plan form similar to current RJ's. Its design features included a swept high wing, and upper surface blowing (USB). There are two reasons that a high wing configuration was chosen. The first reason was to lessen the chance of foreign object damage (FOD) during the wildfire support mission when landing on a semi-prepared runway. The other reason is that the main spar would be allowed to pass completely over the fuselage uninterrupted, thus adding to the structural integrity of the wing.

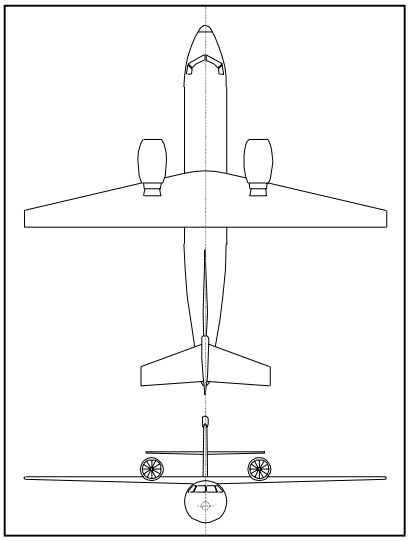

Figure IV.1: Design One

2. Design Two

Design Two, illustrated in Figure IV.2, is similar to Design One. The major differences between the two designs are the canards, externally blown flaps (EBF), and the third engine capable of vectoring thrust. The canards were included initially to decrease the size of the horizontal tail, aiding pitch control, and to decrease the chance of the wing stalling. EBF functions much the same as USB from the previous design in such that they both provided additional lift during takeoff and landing. The third engine was equipped with a thrust-vectoring nozzle to gain an additional increment of lift during takeoff and landing.

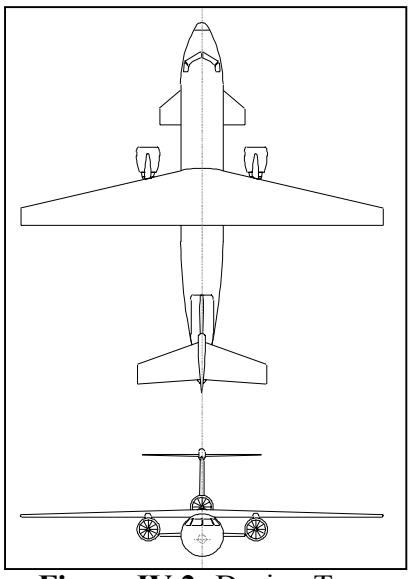

Figure IV.2: Design Two

3. Design Three

Design Three, illustrated in Figure IV.3, was very different from the other two designs and was considered to be the unconventional solution. The primary features of this design were a mid-wing configuration with canards, tail booms, a twin T-tail, and a third engine capable of thrust vectoring. The mid-wing configuration was selected because of

its increase in aerodynamic efficiency. In the wildfire mission, it is probable that the aircraft will be flying over a fire at which time it would see increased turbulence due to the large mass of rising air; the canards and twin T-tail would be beneficial for the increased control compensation needed during both this and slow speed flight. The tail booms were chosen as a solution for attaching the tail structure to the aircraft. The vectored thrust from the third engine would provide extra lift needed for takeoff along with a conventional set of flaps.

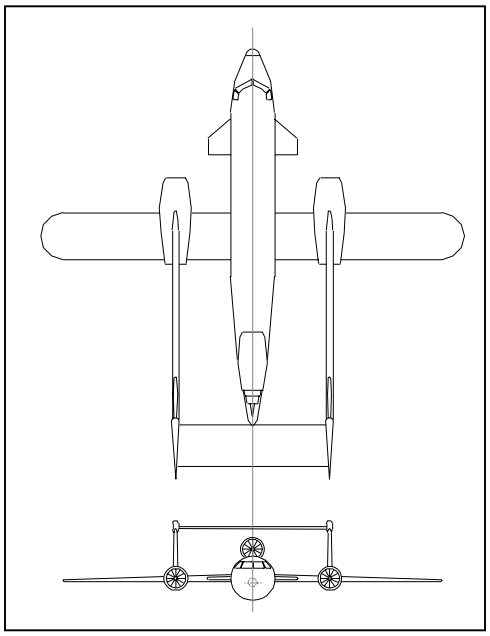

Figure IV.3: Design Three

V. Selection Process:

Further analysis of the three design candidates and their critical issues dictated that selection criteria were needed. These criteria were then used in a Figure of Merit (FOM) to evaluate and select a concept for a more detailed design. The criteria used were: Takeoff Gross Weight (TOGW), Reliability, Mechanical Complexity, Drag Coefficient (C_D), Operational Cost, Flyaway Cost, Upgrade Cost, and Modification Cost. The FOM used is shown below in Table V.1.

Table V.1: Figure Of Merit

	Weight	Design 1	Design 2	Design 3
TOGW	5	4	3	2
Reliability	8.5	4	3	3
Mechanical Complexity	10	4	3	2
C_D	8	4	3	1
Operational Cost	9	4	3	3
Flyaway Cost	4	4	3	3
Upgrade Cost	4	4	3	2
Modification Cost	7	4	4	2
		222	173.5	124.5

By weighting each of the factors we hoped to demonstrate their importance in the evaluation of the designs with ten being the most important and one being the least important. The selection of a particular numerical representation for each factor in the designs was determined by the group members and then averaged to get the values used in Table V.1. The scale used was a one to five scale, where five is the best and one is the worst. The remaining portion of this chapter will be separated into sections discussing the reasons for choosing the particular ratings for each of the designs.

1. Takeoff Gross Weight (TOGW)

The critical area for this particular factor was number of engines. Because both Design Two and Design Three had a third engine, it was determined that they would incur a weight penalty. The reason that Design Three is rated as the lowest is due to the boom structure that extends from the engine nacelles to the tail since it would result in an increased weight due to the fact that it would require additional strength in both the booms and the wing.

2. Reliability

The critical areas involved in this factor are the incorporation of new technologies and the incorporation of a potentially difficult part to design. The first point to consider is the type of high lift system used. Whether using a thrust vectored engine or blown flaps, both require a particular design to undergo a significant amount of testing to prove the reliability of the system. All three of the designs used one of the above-mentioned methods for generating high lift; therefore none could receive a perfect score. In addition to the high lift system, the incorporation of canards required Design Two and Design Three to receive a demerit because they have been shown to be difficult to properly design without extensive testing.

3. Mechanical Complexity

Much of this particular factor's critical areas are the same as those of the above reliability section and are due to the use of high lift systems. Canards caused Design Two and Design Three to receive additional demerits from Design One.

4. Drag Coefficient (C_D)

Basic research was combined with common sense to evaluate each design, to make an informed decision as to which design would have the highest drag. It was determined that the addition of a canard would cause a substantial amount of drag to be incurred on both the canard itself and all things downstream in its vortex. The additional wetted area resulting from the third engine used in Design Two and Design Three causes a substantial increase in drag and therefore merited a demerit. For Design Three, an additional demerit was incurred due to increase in drag from the wetted area of the booms.

5. Operational Cost

This factor is the cost that would be incurred during normal operation and maintenance. The critical part for this factor again came in the way of the third engine and the additional cost stemming from it being overhauled and from the additional fuel it would use in flight. This caused both Design Two and Design Three to be given a demerit.

6. Flyaway Cost

This factor is the cost that a company would pay for the initial purchase of the aircraft. The only critical area for this was the inclusion of the third engine in Design Two and Design Three.

7. Upgrade Cost

This factor involves the cost of an upgrade between series of aircraft for instance, if a company wanted to upgrade from the –200 series to the –300 series. For Design One, this would prove to be a relatively easy process, as only the wing and fuselage need modification. For both Design Two and Design Three the third engine would have to be taken into account with the possibility of a modification to it. Lastly, for Design Three, in addition to the above-mentioned upgrades, the booms leading to the tail would also have to be extended.

8. Modification Cost

This factor involves the adaptation of the primary design to the secondary mission as a wildfire support aircraft. Because of the relatively conventional design of the fuselage for both Design One and Design Two, the modifications to these would be cheaper than the modification to Design Three. Design Three requires special consideration because of the tail booms when placing any sort of cargo door.

9. Final Selection Of The AAT

With the above sections in mind, Table V.1 was created and each of the group members evaluated the three initial designs. It was decided that Design One would be investigated in further detail.

VI. Aircraft Layout:

One of the key points considered in the development of the aircraft layout was the impact of modifying the aircraft to fulfill both the primary and secondary missions. The philosophy reached is that, in the initial purchase phase, the airline company must make the decision as to whether or not they would like their aircraft to be capable of performing both missions. If they decide that they would like to perform both missions, the production company would use an entirely different set of internal blueprints from an aircraft capable of only the primary mission. This was done to better emphasize the cost differential that the government would subsidize. It should be known that none of the wildfire mission specific accommodations or systems are included in the cost of an aircraft that performs strictly the primary mission nor does the cost allow for the later modification of an aircraft to perform both missions.

In an effort to reduce the cost of the aircraft to both the airline company and the government, the use of advanced technologies was limited to that which has been proven through use on a working aircraft.

1. Initial Fuselage Sizing

The size of the fuselage was dictated by four factors; cockpit length, cabin length, baggage area, and aerodynamic feathering. The cabin length was dictated by both the seat pitch and the number of seats needed, yielding a cabin of roughly 9 ft by 40 ft. After calculating the total volume of baggage for the maximum load of passengers, adding in the standard length of the cockpit, and aerodynamic feathering to the fuselage, the total

length was calculated to be 80 ft. Through the examination of comparator aircraft dimensions, the width of the fuselage was decided to be 10 ft.

2. Primary Mission Cabin Design

The overall dimensions of the cabin are 9 ft by 40 ft and are shown in Figure VI.1. It features a galley and attendant's seat located in the forward section of the cabin, and a lavatory and storage compartment in the aft section. There are 50 passenger seats arranged in a 2 by 2 configuration with a 2 ft aisle running the length of the cabin between them. The rows have a seat pitch of 34 in except for the emergency row which has a seat pitch of 36 in. The emergency exit doors are located after the sixth row of seats.

3. Wildfire Support Mission Cabin Design

For the wildfire support mission, the location of the galley, storage area, and lavatory remain the same, as it is not cost effective to change them, see Figure VI.1. An oversized door was added in the aft section of the plane and a rolling track with a width of 2 ft was also added to aid the movement of the fire suppressant and any equipment during loading and unloading. The fire suppressant is marked on the drawing by the crosshatched area and measures a length of 10 ft. Bench seats run for 22.5 ft along the outer portions of the cabin and were dimensioned to house the fire suppressant.

4. Converting From Primary To Wildfire Cabin Layouts

The act of interchanging the various accommodations was designed to be a simple one. The first step to converting the cabin is the removal of all primary seating and overhead storage compartments. This is made possible through the use of quick release mechanisms on each component. In addition to this, the panels that cover the rear cargo door must be removed. Next, the bench seats and the harnesses that will be used by the firefighters must be installed implementing the same quick release system. The last step is to strap the suppressant tanks under the rear seats and to uncover the rollers by removing the rubber mat that is the aisle for the primary mission.

To load and unload the suppressant, it is assumed that a pumping system will be available at both the airport and the landing zone. Also, to aid in the addition and removal of accommodations and to aid in the addition of supplies and equipment, a ramp will be stowed in the rear cargo bay and will attach to the bottom of the cargo door.

5. Upgrading To –200 Or –300 Aircraft

It was specified in the RFP that the aircraft must have the capability of being upgraded from the –100 series to two subsequently larger versions, the –200 and –300 series, which are required to hold at least 65 and 81 passengers respectively. The philosophy adapted for the AAT is shown in Figure VI.2 and includes one extra seat on each subsequent series. Fuselage plugs will be added on either side of the wing to prevent instability.

PRIMARY

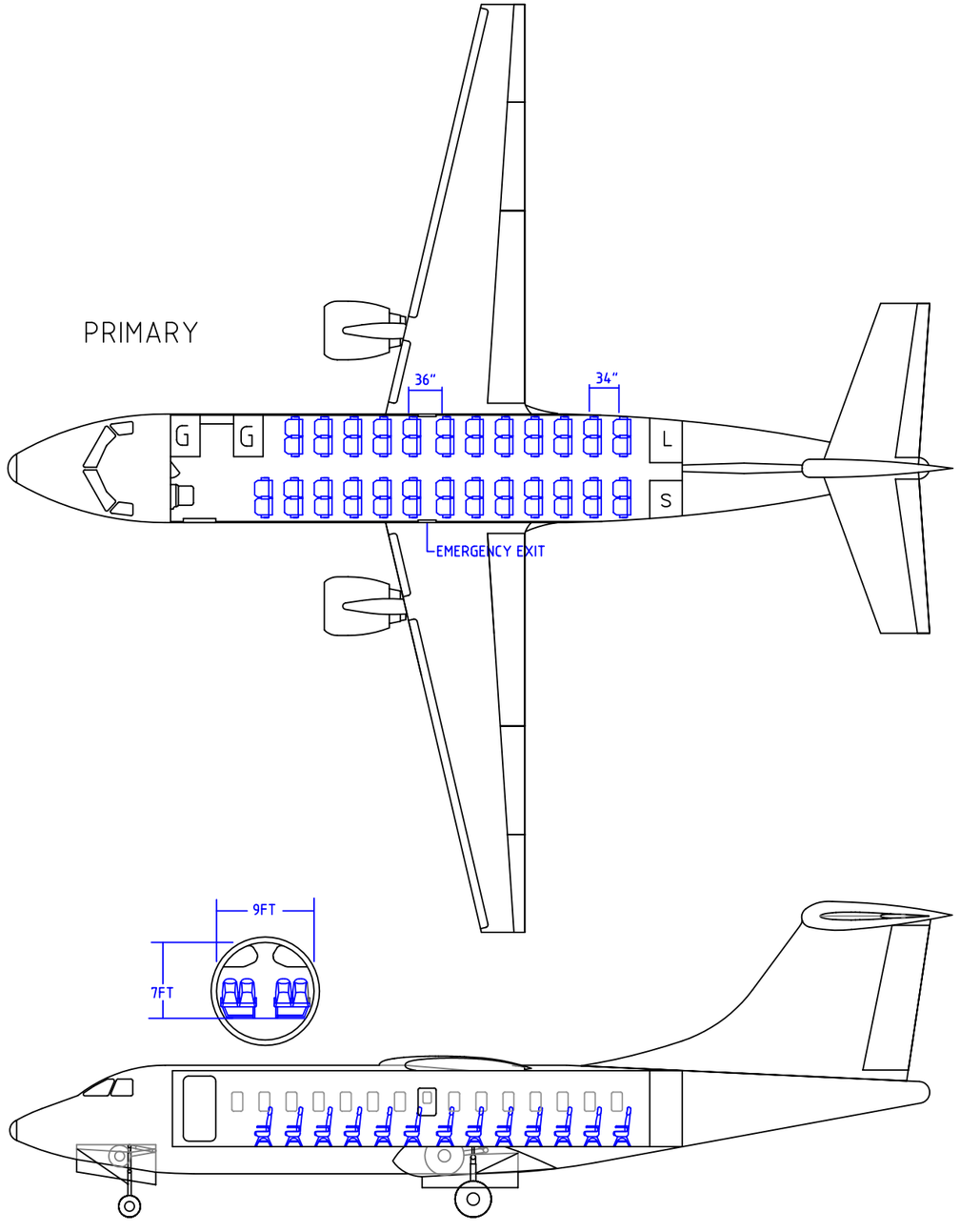

SECONDARY

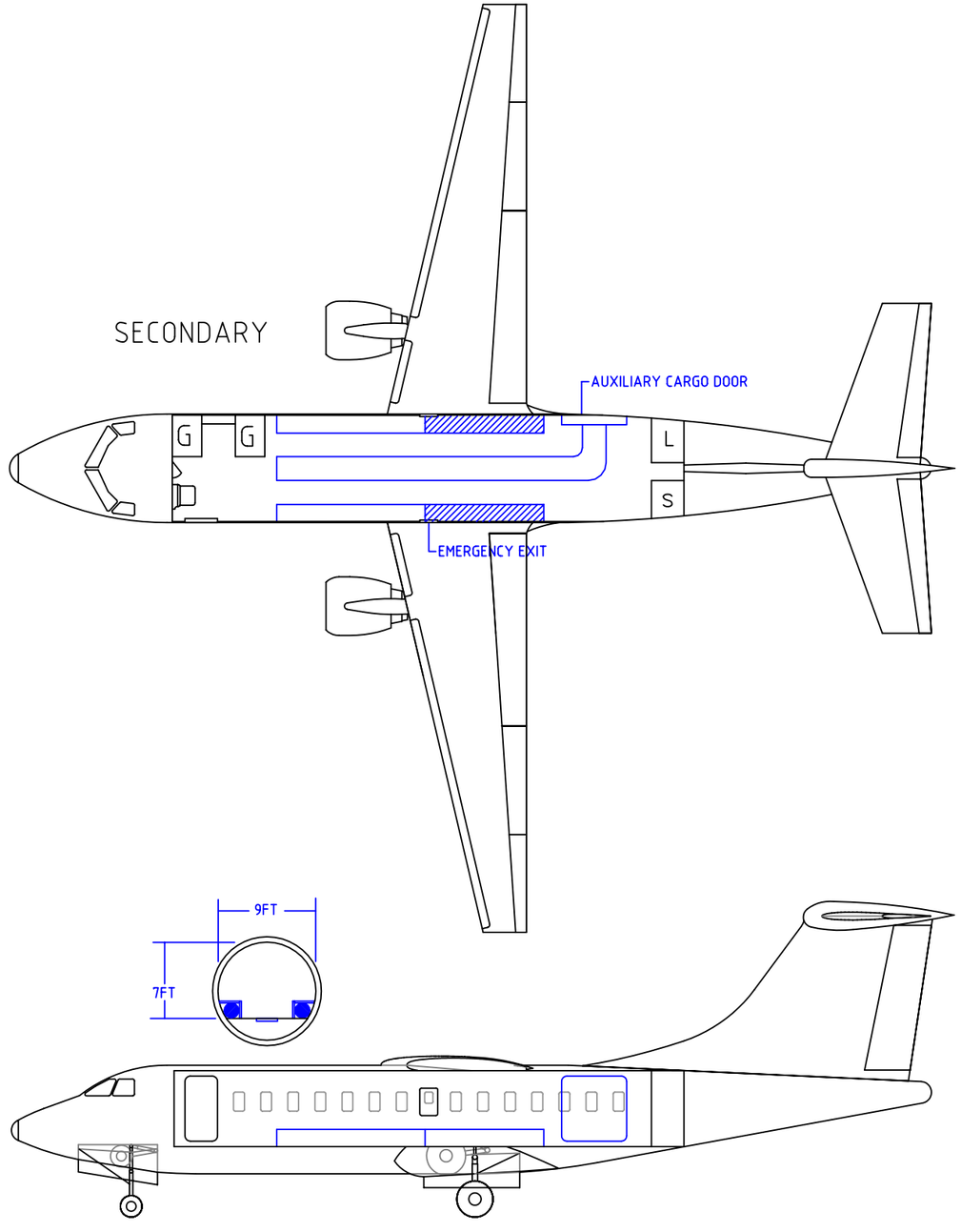

SCALE (FT)

0 10 20 30 40

TEAM BACCHUS	
INBOARD PROFILE (PRIMARY AND SECONDARY)	AIRCRAFT MODEL: AAT-100
	DRAWING VERSION: 1.1
	REVISON DATE: 5/3/2004 M.T.

Figure VI.1: Inboard Profiles For Primary And Secondary Mission

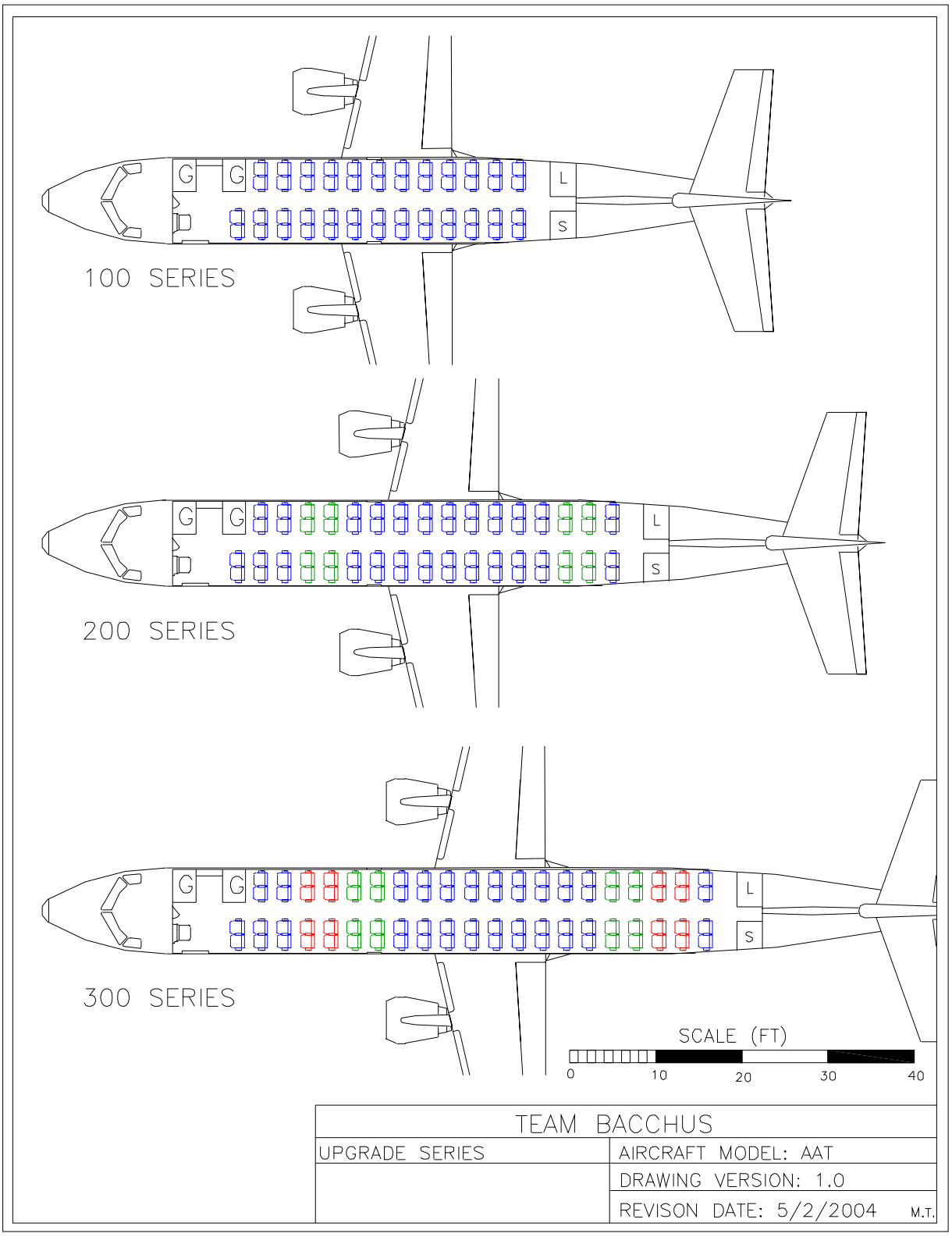

Figure VI.2: Upgraded Seating Arrangements For –200 And –300 Aircraft

VII. Weight Estimation:

At an early stage of the design process, it was important to estimate the TOGW since it was shown to be a project driver for all missions. Initial calculations were done using a weight fraction method found in Reference 2. The method used is an iterative process that requires an initial "guess" and was considered converged when the initial estimation and the final weight were within 0.04% error. Using this method, TOGW for the primary mission was determined to be approximately 52,600 lbs.

VIII. Constraints:

To better define a feasible range of values and to provide some initial numbers to be used in the analysis of the AAT, a carpet plot was developed using the equations outlined in Reference 2. The relationship between thrust-to-weight ratio (T/W) and wing loading (W/S) was plotted for the primary mission and is illustrated below in Figure VIII.1.

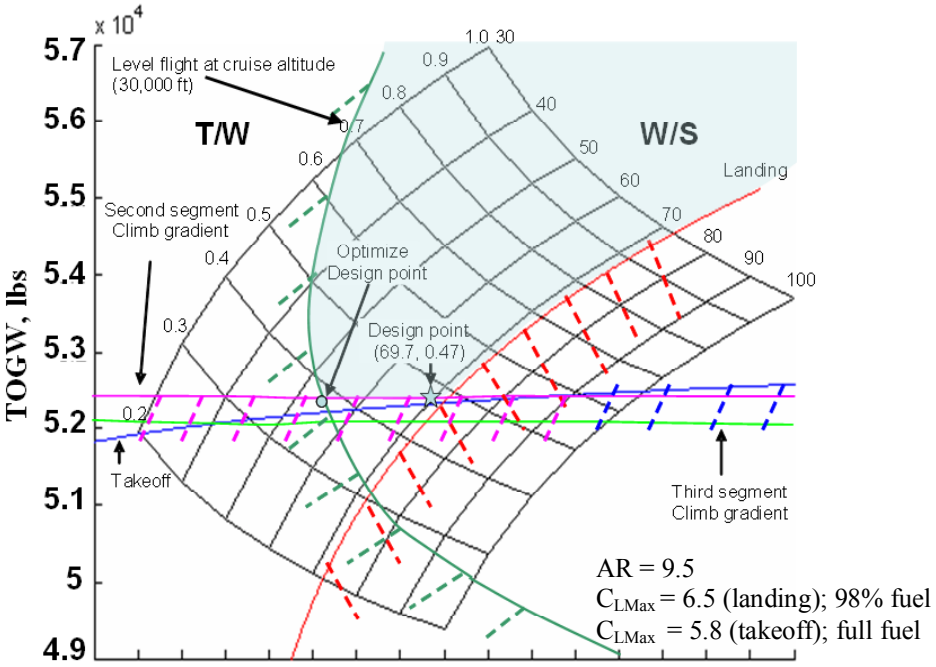

Figure VIII.1: Primary Mission's Carpet Plot

To narrow the feasible region, shown in green on Figure VIII.1, the takeoff, landing, second, and third segment lines were calculated for a hot day at Denver's altitude and the wing loading and thrust-to-weight ratios for each of the segments were converted to the sea level condition. Normally, for this type of carpet plot, the optimized design point would be given by the intersection of the takeoff constraint and the climb gradient constraint. However, for the AAT, it was determined that if the optimum point

was used then the wing loading would be too low, indicating a large wing area and a 20% higher drag. Therefore, the design point for the AAT was selected to be the where the W/S was 69.7 and T/W was 0.47.

From this carpet/constraint case study, the minimum required C_{LMax} for landing was calculated by reducing the C_L until the design point was in the infeasible regime. It was found that the minimum C_L was 6.5. Since the primary mission required a BFL of 2500 ft with one engine inoperative, our aircraft design will be required to meet this minimum required C_{LMax} with mechanical flap deployment and partial powered lift. For the wildfire mission it will not be possible to land with a BFL of 2000 feet if one engine is inoperative. The RFP did not require this condition to be fulfilled, so it is assumed that the aircraft would divert.

1. Center Of Gravity (CG) Calculation

After the initial takeoff gross weight was determined, a series of statistical equations from Reference 2 were used to calculate the weight of each of the components of the aircraft. By using the initial TOGW of 52,600 lb, and the equations in Reference 2, a more accurate estimate was computed. The resulting component weights for each mission are shown in the tables included on Figure VIII.2. The gross weight for the wildfire mission was determined to be 3090 lbs less than the primary mission and stems from the reduction in the amount of the total payload. As a result, it is possible to carry an additional 3000 lbs of fire suppressant or light equipment although an adjustment of the CG will be required.

Primary mission	weight, lbs	x cg, in.	z cg, in.	x-moment, lb-in	z-moment, lb-in
Structure					
wing	4888.63	418.80	170.00	2047358.11	831067.04
horizontal tail	566.43	935.16	340.00	529700.66	192585.47
vertical tail	525.57	893.07	225.00	469368.93	118252.46
fuselage	9087.55	462.00	125.00	4198446.92	1135943.43
main landing gear	709.02	512.40	50.00	363302.55	35451.07
nose landing gear	206.38	132.48	48.00	27340.60	9906.01
Propulsion					
engine	4670.00	370.00	125.00	1727900.00	583750.00
nacelle group	576.73	370.00	126.00	213388.74	72667.52
engine controls	30.00	378.60	60.00	11358.00	1800.00
Systems					
starter	116.73	378.60	60.00	44194.04	7003.81
fuel system	393.60	428.00	60.00	168462.32	23616.21
flight control	949.79	516.80	170.00	490852.90	161464.64
instrument	169.19	172.80	90.00	29235.60	15226.87
APU installation	1515.00	420.00	60.00	636300.00	90900.00
hydraulics	199.94	416.00	60.00	83176.84	11996.66
electric	629.55	91.80	85.00	57792.59	53511.66
avionics	1235.33	102.00	85.00	126003.83	105003.19
furnishings	507.33	720.00	100.00	365274.12	50732.52
air conditioning	908.76	936.00	140.00	850600.73	127226.60
anti-ice	124.00	900.00	140.00	111600.00	17360.00
handling gear	15.60	96.00	120.00	1497.60	1872.00
seat (crew)	195.00	128.40	110.00	25038.00	21450.00
seat (passenger)	3185.00	480.00	100.00	1528800.00	318500.00
empty weight	31405.12	449.19			
Miscellaneous					
fuel	10192.00	430.00	170.00	4382560.00	1732640.00
crew	690.00	128.40	125.00	88596.00	86250.00
payload	9065.00	480.00	110.00	4351200.00	997150.00
baggages	1575.00	480.00	150.00	756000.00	236250.00
baggages in cargo	630.00	798.00	125.00	502740.00	78750.00
total	53557.12			24188089.06	7118327.17
C.G location from nose/ground, in.				**451.63**	**132.91**

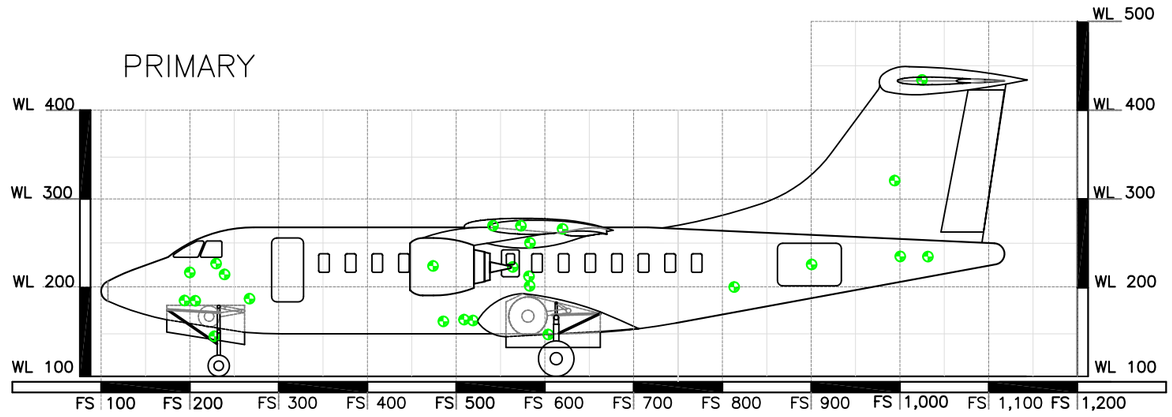

Secondary mission	weight, lbs	x cg, in.	z cg, in.	x-moment, lb-in	z-moment, lb-in
Structure					
wing	4888.63	418.80	170.00	2047358.11	831067.04
horizontal tail	566.43	935.16	340.00	529700.66	192585.47
vertical tail	525.57	893.07	225.00	469368.93	118252.46
fuselage	9087.55	462.00	125.00	4198446.92	1135943.43
main landing gear	709.02	512.40	50.00	363302.55	35451.07
nose landing gear	206.38	132.48	48.00	27340.60	9906.01
Propulsion					
engine	4670.00	370.00	125.00	1727900.00	583750.00
nacelle group	576.73	370.00	126.00	213388.74	72667.52
engine controls	30.00	378.60	60.00	11358.00	1800.00
Systems					
starter	116.73	378.60	60.00	44194.04	7003.81
fuel system	393.60	428.00	60.00	168462.32	23616.21
flight control	949.79	516.80	170.00	490852.90	161464.64
instrument	169.19	172.80	90.00	29235.60	15226.87
APU installation	1518.00	420.00	60.00	637560.00	91080.00
hydraulics	199.94	416.00	60.00	83176.84	11996.66
electric	629.55	91.80	85.00	57792.59	53511.66
avionics	1235.33	102.00	85.00	126003.83	105003.19
furnishings	504.33	720.00	100.00	363114.12	50432.52
air conditioning	908.76	936.00	140.00	850600.73	127226.60
anti-ice	124.00	900.00	140.00	111600.00	17360.00
handling gear	15.60	96.00	120.00	1497.60	1872.00
seat (crew)	195.00	128.40	110.00	25038.00	21450.00
seat (passenger)	1300.00	480.00	100.00	624000.00	130000.00
thermal sensing device	200.00	798.00	125.00	159600.00	25000.00
empty weight	29720.12	449.56	128.66		
Miscellaneous					
fuel	10192.00	430.00	170.00	4382560.00	1732640.00
crew	690.00	128.40	125.00	88596.00	86250.00
payload	3300.00	480.00	110.00	1584000.00	363000.00
baggages	2880.00	480.00	110.00	1382400.00	316800.00
fire suppressant	2000.00	552.00	95.00	1104000.00	190000.00
additional(ATV)	0.00	504.00			
total	48782.12			21902449.06	6512357.17
C.G location from nose/ground, in.				**448.99**	**133.50**

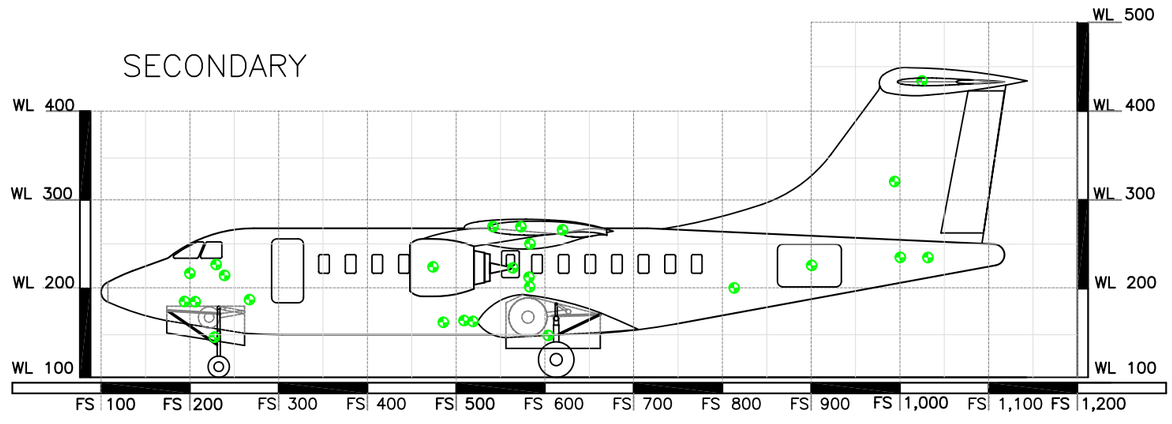

TEAM BACCHUS	
COMPONENT CG LOCATION	AIRCRAFT MODEL: AAT-100
	DRAWING VERSION: 1.2
	REVISON DATE: 5/6/2004 M.T.

Figure VIII.2 : Component CG Location

2. CG Mission Envelope

The CG location of the aircraft structure was determined by summing the moments and then dividing by the gross weight yielding it to be 451.6 in from the nose of the aircraft or 22.3% mean aerodynamic chord (MAC) for the primary mission, and 449.0 in or 20.1% MAC for the secondary mission.

Figure VIII.3 shows the CG travel of a typical primary and secondary mission with the forward and aft limits determined from the relation of stability to wing geometry and outlined in Chapter XII later. Table VIII.1 and VIII.2 show the segment summaries for both missions. Examining the preliminary results of the CG envelope, an additional weight of 200 lbs was required to maintain the stability of the aircraft during takeoff for the wildfire mission. This was due to the decreased weight of the secondary mission and was solved by placing a thermal sensing device in the aft-most part of the fuselage.

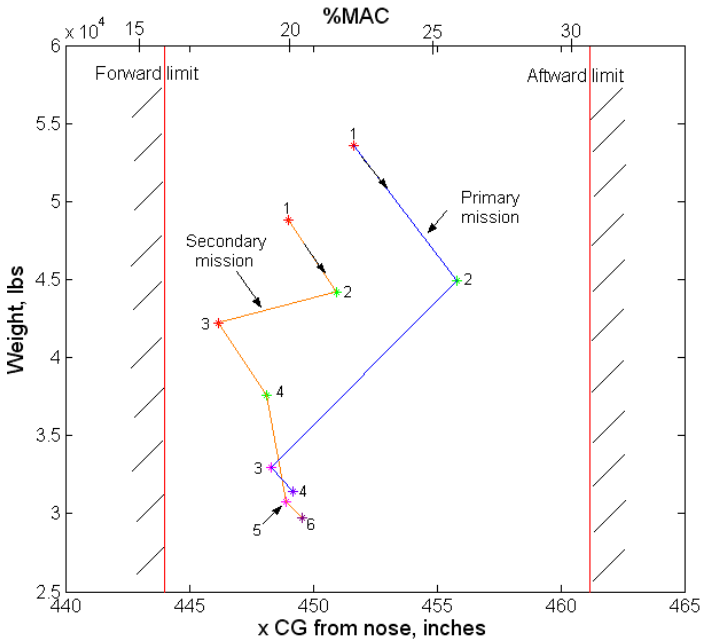

Figure VIII.3: CG Envelope For Primary And Secondary Missions

Table VIII.1: Primary Mission Envelope Points

Segment	Primary Mission	Weight (lbs)	CG (% MAC)	CG (in from nose)
1	Takeoff (Full load)	53,557	22.3	451
2	Landing (15% fuel remaining)	44,893	26.1	455
3	Exit passenger	32,933	18.9	448
4	Empty weight	31,405	20.2	449

Table VIII.2: Secondary Mission Envelope Points

Segment	Secondary Mission	Weight (lbs)	CG (% MAC)	CG (in from nose)
1	Takeoff (Full load)	48,782	20.1	449
2	Landing (55% fuel remaining)	44,195	22.3	451
3	Re-takeoff (without 2000 lb of suppressant)	42,195	16.7	446
4	Landing (20% fuel remaining)	37,609	19	448
5	Exit passenger baggage	30,739	20.2	449
6	Empty weight	29,720	20.6	450

IX. Propulsion Requirements And Considerations:

Due to the RFP requirements of a BFL that is 40-50% less than that of a comparator aircraft, the design of the propulsion system was particularly important. The most important factors for evaluating a particular propulsion system were safety, cost and the ability to meet the performance requirements with the less important factors being reliability, maintainability, and operational expenses. Careful consideration of these six factors was necessary to properly design an aircraft that could be safely and efficiently flown and successfully marketed to investors. The remainder of this section of is dedicated to the details of the engine configuration as well as the engine selection process.

1. Two Engines Vs. Three Engines

The three initial design configurations had either two or three engines. The three-engine configuration was eliminated after considering cost, safety, and information contained in the YC-14 case study. In that report, Boeing showed that twin-engine aircraft have been statistically safer than aircraft using four engines, although no reason is given for the increased safety. Twin-engine aircraft have a significant cost advantage, are less complex, and require less maintenance than similar aircraft with three or more engines.

Since the FAA requires that the aircraft be able to fly in the event of an engine loss, a twin-engine aircraft must have twice the power necessary to fly while other aircraft must have $\frac{100n}{(n-1)}\%$, where n is the number of engines. Another direct cause of this requirement is that a twin-engine design has 100% more power available for

maneuvering versus the $\left[\frac{n}{(n-1)}-1\right]100\%$ more power available for an aircraft with three or more engines.

Another difference in the designs is that an increase in the number of engines yields an increase in the weight and ram-drag during flight. Probably one of the most important differences in the designs is that it is cheaper to purchase two more powerful engines than it is to purchase three less powerful engines. Based on this, a twin-engine design is the most cost effective.

2. Engine Decks And Performance Data

Engine data was provided by the AIAA for unspecified versions of the General Electric CF 34 and the General Electric / SNECMA CFM 56. Comparisons with data obtained off the GE and SNECMA websites and those found in *Jane's Aero-Engines* (Ref. 9) suggested that the data was for de-rated versions of the CF 34-3 and the CFM 56-3B2. Several models of each engine were investigated to determine which was best suited for our RJ. It was determined that the data provided for the CF 34 was inconsistent with data obtained elsewhere and therefore the data from the CFM 56 was scaled to model the CF 34.

3. General Electric CF 34

The CF 34 engine, illustrated in Figure IX.1**,** is well known in the aircraft industry because it is used on the majority of all the RJ's. It is available in max thrust ranges of 9220 lbs to 18,500 lbs at weights ranging from roughly 1500 to 4000 lbs. The most powerful variant is the CF 34-10E and is rated at 18,500 lbs of thrust. Two CF 34-10E

engines can provide for a max T/W = 0.46 for an RJ weighing 80,000 lbs. This suggests that the higher end model variants of the CF 34 are powerful enough to work on all future models of the AAT.

Figure IX.1: GE CF 34 (Ref. 16)

4. General Electric / SNECMA CFM 56

The CFM 56 engine, illustrated in Figure IX.2, is found mainly on mid-size jets such as the Boeing 737 and Airbus A3XX series, as well as on some military aircraft. Like the CF 34, it has proven its reliability and safety throughout the years and continues to be upgraded and used on newer planes. The CFM 56 comes in variants with max thrusts ranging from 18,500-34,000 lbs and weights varying from roughly 4300-8800 lbs. From the data available it appears that several variants of the CFM 56 have better specific fuel consumptions (SFC) at cruise than many of the CF 34 variants. However, the CFM 56 on average weighs more and provides significantly more thrust than is needed for our RJ to the point where it becomes excessive for all models.

Figure IX.2: GE / SNECMA CFM 56 (Ref. 17)

5. Engine Selection

After examining the engines listed in Table IX.1, a twin-engine configuration was chosen using the CF 34-8C1 for the initial 50 passenger version. One engine has a maximum thrust in excess of 12,670 lbs available at takeoff while two of these engines combined to bring the thrust available to 25,340 lbs. Power available can be read off of the engine deck shown below in Figure IX.3 which details the maximum thrust versus altitude and Mach number.

Table IX.1: GE CF 34 Engine Data (Ref. 9)

Engine Model	Thrust (lb)	Weight (lb)	Diameter (in)
CF34-8C1	12670	2335	52
CF34-8D1	12500	2470	52
CF34-8D3	14500	2470	52
CF34-8E	14500	2470	52
CF34-10E	18500	3800	57

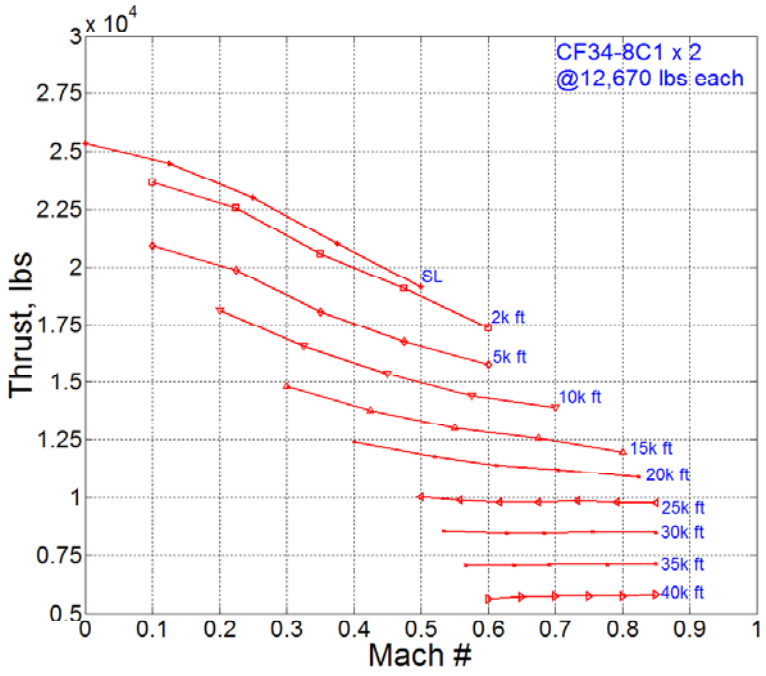

Figure IX.3: Thrust Vs. Mach Number For Two CF34-8C1 Engines

X. Aerodynamics:

As was stated earlier, C_{LMax} was dictated by the landing constraint and was calculated to be 6.5. This section mainly deals with the specific geometric decisions that were made in the development of this lift coefficient however a portion is dedicated to drag polars.

1. Wing Sizing

Using the carpet plot shown in Figure VIII.1, the chosen design point had a wing loading of 70 lbs/ft^2. From this wing loading and the TOGW, a wing area (S) of 769.5 ft^2 was obtained. Early on in the design process, the aspect ratio (AR) and root chord (c_r) were fixed at 9.5 and 14 ft respectively. These were chosen based on the scale of comparator aircraft and allowed for us to derive all of the dimensions shown below in Table X.1 by using only the standard equations for AR.

Table X.1: Final Wing Dimensions

	Dimension	Units
AR	9.5	
c_r	14	ft
S	769.5	ft^2
c_t	4	ft
c_{bar}	9	ft
b	85.5	ft
λ	0.29	

2. Drag Divergent Mach Number (M_{DD})

After shaping the wing to fit the aforementioned constraints, the next step was to lessen the AAT's transonic drag. To accomplish this, the sweep of the leading edge (LE) was increased gradually and the behavior of the drag divergent Mach number (M_{DD}) was

examined. M_{DD} is the Mach number at which the aircraft's drag experiences a rapid increase. This can become a critical factor in limiting how high of a speed an aircraft can achieve in the cruise condition. Although LE sweep delays drag rise, it tends to create both structural and aerodynamic issues. From a structural point of view, adding sweep adds more structure per span, and therefore more weight per span. From an aerodynamic point of view, if a wing is swept aft, it tends to make the tips stall quicker than the roots. This however, can be remedied through the use of wing twist or washout.

The Korn equation, shown below, was used to analyze the Mach number where the drag rise occurs. This equation gives M_{DD} as a function of the sweep angle (Λ) of the wing, the local airfoil's lift coefficient (C_l), the thickness ratio (t/c) and the airfoil technology factor (K_a). The airfoil technology factor was given as 0.95 as a supercritical airfoil was decided upon for if cruise efficiencies at transonic speeds. A thickness ratio of 12% was chosen. This was given mainly as a function the of volume of fuel and structure required in the wing.

$$M_{DD} = \frac{K_a}{\cos\Lambda} - \frac{t/c}{\cos^2\Lambda} - \frac{C_l}{10\cos^3\Lambda} \qquad (1)(\text{Ref. } 18)$$

Using equation 1, the effects of changing the lift coefficient were examined. From this study, and a list of available airfoils with such coefficients, it was found that a design lift coefficient of 0.7 was the optimum available. Using these values, Figure X.1 was developed and shows that the wing for this particular design does not need to be swept at all to attain the minimum velocity. However, if some sweep is added the benefits are an increase in speed. After consulting with the structural personnel for the AAT, it was determined that if the wing sweep were kept at a small enough angle it would not cause a dramatic increase in structural weight. It was decided that sweeping

the LE at a 13 degree angle was beneficial because the aircraft could attain a maximum speed of 425 kts with a 5% safety margin.

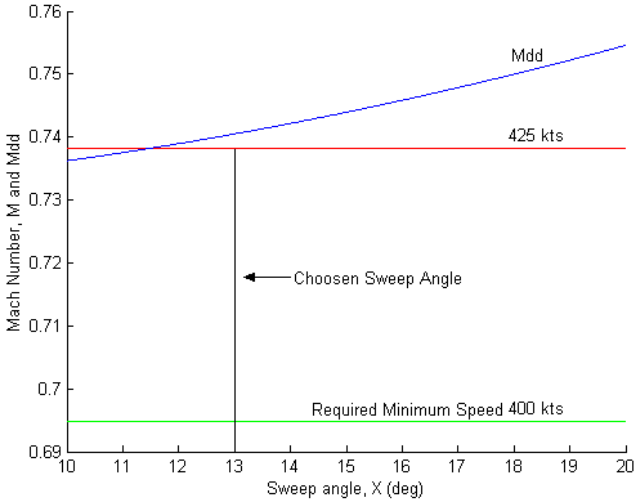

Figure X.1: M_{DD} And The Required Minimum Speed

3. Airfoil Selection And Maximum Clean Lift:

The primary method of airfoil selection was based on a trade-off study during the investigation into M_{DD}. It was determined from this that a reasonable combination of effects was the use of a supercritical airfoil with a C_l of 0.7 and a t/c of 12%. After designating the basic criteria of the airfoil, a NASA SC(2)-0712 was chosen and is shown below in Figure X.2. It has a design C_l of 0.7 and a t/c of 0.12. Using a program called XFOIL, the lift curve shown in Figure X.3 was developed. A quick note should be made that after running a test case of two NACA 4-series airfoils and comparing them with the plots in Reference 9, it was determined that XFOIL over predicts the maximum lift by 10%. The results of the XFOIL program and subsequent correction factor are shown below Figure X.3.

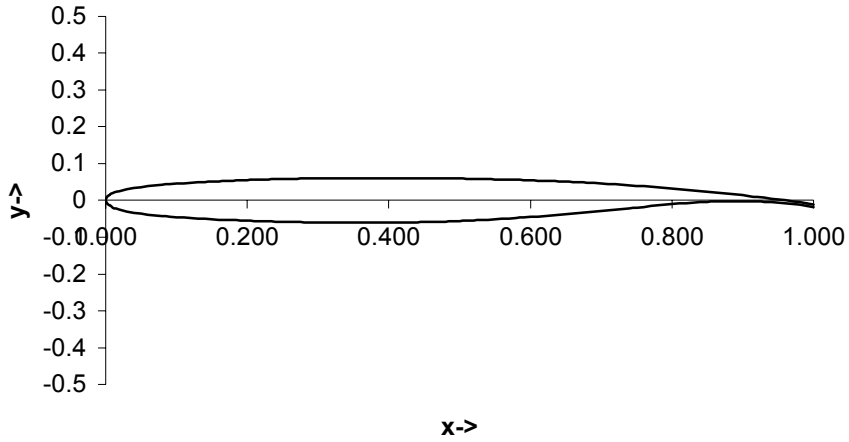

Figure X.2: NASA SC(2)-0712 Airfoil Cross Section

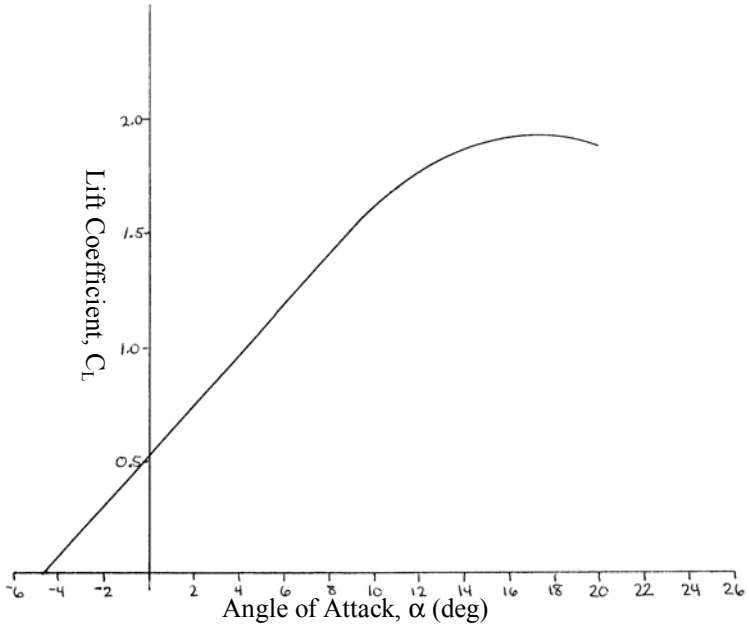

Figure X.3: Lift Curve For NASA SC(2)-0712 At Mach 0.7

From XFOIL, the maximum lift was calculated to be 2.2, but when a 10% correction factor was implemented, the maximum lift of the airfoil was given as 1.9.

3. Determining The Maximum Clean Lift Of The Wing

After an airfoil was selected, various methods were applied to the data to obtain the lift curve for the full wing.

$$C_{LMax_W} = 0.9C_{l\max}\cos(\Lambda_{c/4}) \qquad (2)(\text{Ref. 2})$$

Using equation 2 shown above, the maximum lift of the wing was found to be 1.9 and using Reference 3 the lift curve slope was found to be 6.4 per radian. This combination of these effects was used to produce the wing's clean lift curve shown below in Figure X.4.

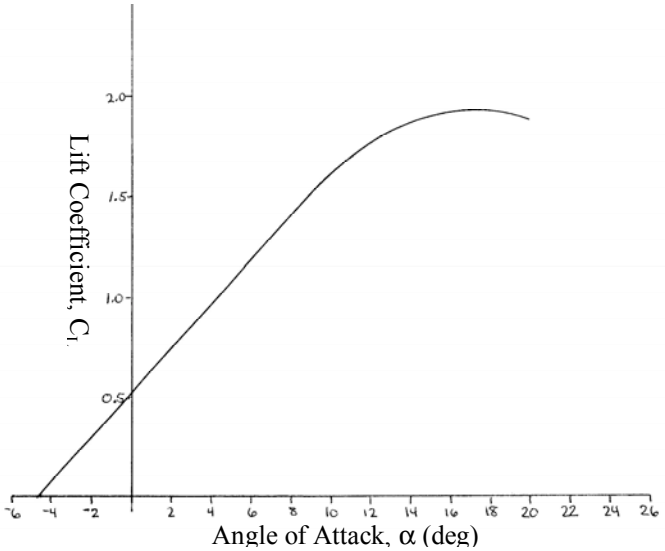

Figure X.4: Lift Curve For The Wing (Clean) At Mach 0.7

4. Drag Developed

The conventional way to visualize the drag developed during a specific mission configuration is through the use of drag polars. The requirement set forth in the RFP was to provide three drag polars, one each for takeoff, cruise, and landing. However, because the takeoff and landing configuration were specifically designed to be the same, only two

drag polars are needed. Figure X.5 below shows the drag attained in the cruise condition. This resulted in a lift to drag ratio of about 19.

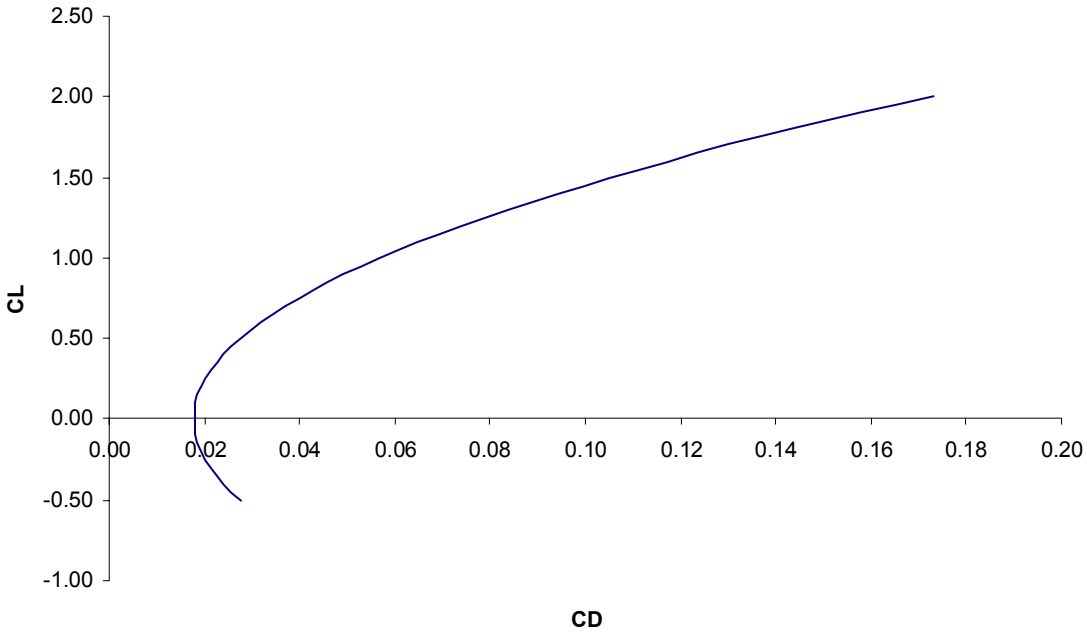

Figure X.5: Drag Polar In Cruise Condition

The landing drag polar was developed using methods outlined in Reference 3 for the subsonic case. This polar illustrates that, when fully deployed, the flap system and the landing gear increase the drag. It should be noted here that the term fully deployed when used in reference to the flaps implies that the trailing edge flaps were deflected to 60 degrees and the leading edge slat was deflected to 10 degrees. Figure X.6 was developed and was shown to decrease our lift to drag ratio to 5.5.

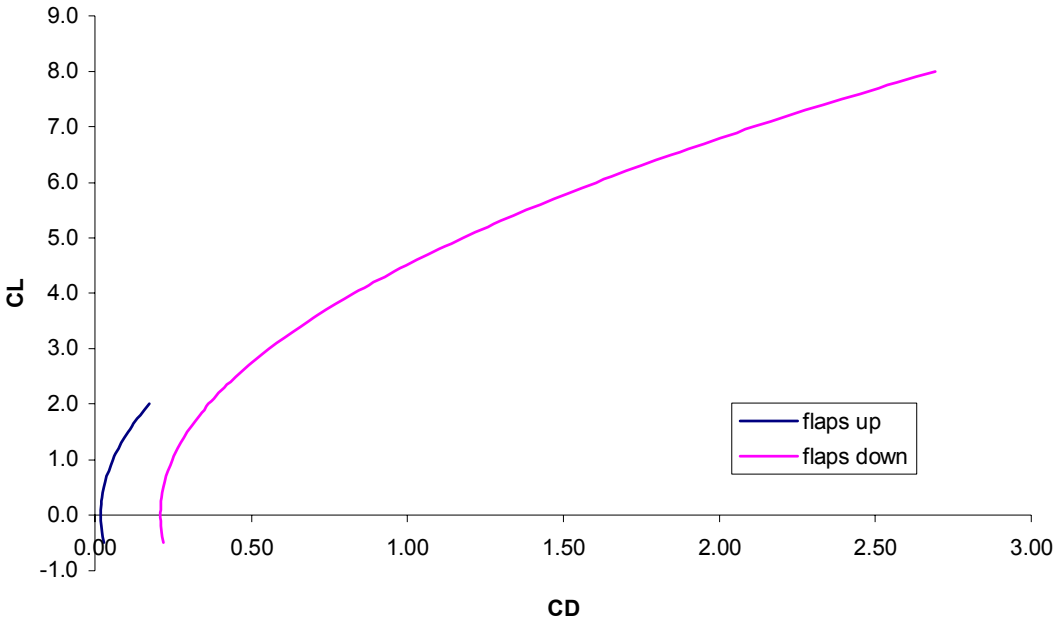

Figure X.6: Drag Polar For Landing And Takeoff Condition

During this investigation, the parasite drag of the major components were tabulated, and are included below in Table X.2.

Table X.2: Parasite Drag For Cruise And Landing/Takeoff Conditions

Component	**Clean**	**Flaps And Gear Deployed**
Wing	0.007147	0.007147
Fuselage	0.007339	0.007339
Horizontal Tail	0.001694	0.001694
Vertical Tail	0.001707	0.001707
Flaps		0.160786
Gear		0.030000
Total	0.017887	0.208673

XI. High And Powered Lift Generation:

As was seen from the previous section on propulsion, several high lift configurations were considered. This chapter examines the use of lift augmentation devices including upper, externally, and internally blown flaps along with the contribution of a mechanical flap system to develop a high lift coefficient.

1. Contribution Due To Mechanical Systems

It was found earlier through the constraint diagram that the driver for both missions for the AAT was the landing constraint. When the C_L was changed to be below 6.5, the design point fell in the infeasible region. In addition, the RFP mentions that in order to perform the landing and be certified, the AAT must be able to complete the SNI landing with one engine out. This means that any contribution due to a powered lift system cannot be fully counted. An investigation into mechanical flap systems was conducted on comparator aircraft and found that most of them used double slotted flap systems on the trailing edge of the wing along with a leading edge slat. This combination of systems was chosen based on the fact that it has already been proven on multiple aircraft.

1.1 Airfoil Lift Curve With Mechanical System

Following the steps outlined in Reference 3, the first step to calculating the three dimensional C_{LMax} with flaps is to calculate their effect on the two dimensional airfoil. The flap configuration shown below in Figure XI.1 was used throughout the process.

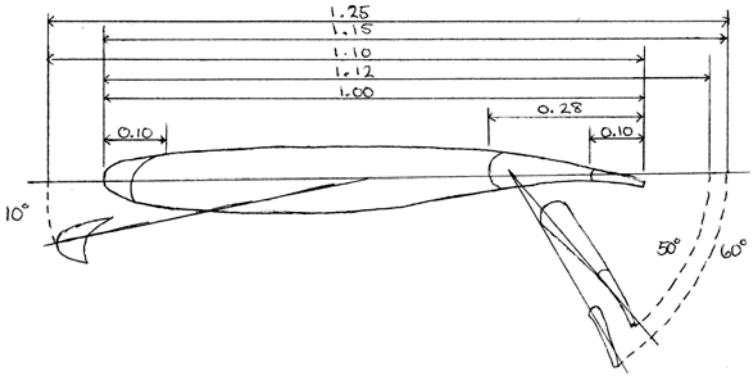

Figure XI.1: 2D Flap Configuration On Airfoil (dimensions in %c)

From this method and geometry, the lift curve shown in Figure XI.2 was made which illustrates that the maximum lift attainable in two dimensions is 4.2.

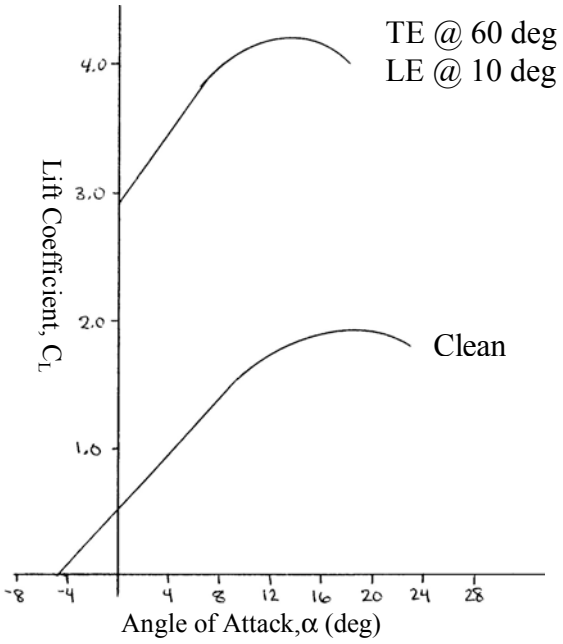

Figure XI.2: Airfoil Lift Curve With Mechanical Flaps

1.2 Wing's Maximum Lift Due To Mechanical Flaps

Using Reference 3 methods again, the lift curve was constructed for the AAT's particular flap system. It should be noted here that it was at this point that both the wing's incidence and the wing's twist was set to 3 degrees and –4 degrees respectively to improve the maximum lift by preventing tip stall. Figure XI.3 shows both the clean and the flapped configuration's respective lift curves.

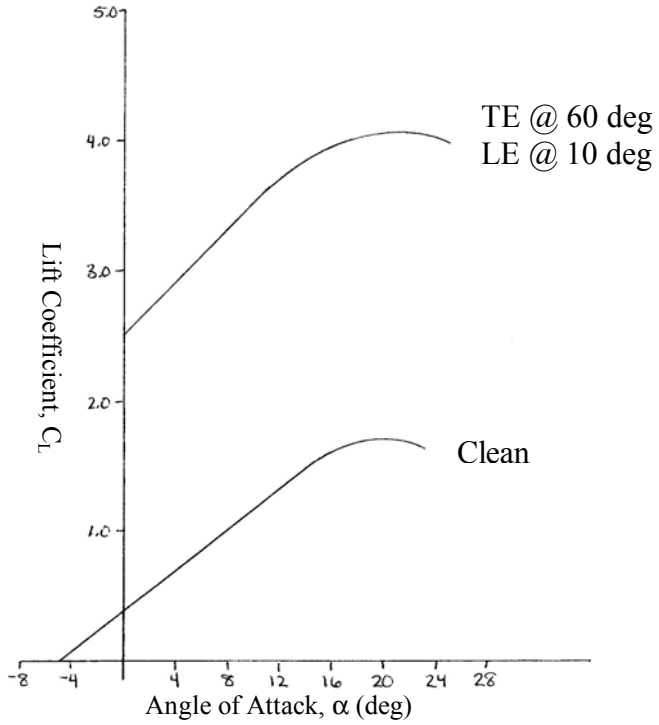

Figure XI.3: Clean And Flapped Wing Lift Curves

As can be seen from the above figure, C_{LMax} for the AAT's flap system is 4.1; primarily due to the fact it has nearly full span double slotted flaps (minus the section dedicated to the flaperons). Even though C_{LMax} is high for this configuration, it is still not high enough to complete the SNI landing without partial blowing.

2. Contribution Due To Powered Lift

2.1. Lift Augmentation System Selection

Several different options for augmenting the maximum lift coefficient at high angles of attack were studied. Of the studied flap configurations employed for typical transport and STOL aircraft, blown flaps raise the lift coefficient the most (Ref. 11). Lift coefficients in excess of 3 and in some cases, such as the NASA QSRA, greater than 10, are achievable through the use of powered lift (Ref. 12). The lift coefficient achieved depends heavily on the amount of flap area that is blown with respect to the wing, thrust, and the mass flow.

Internally blown flaps (IBF), shown below in Figure XI.4, increase the available lift the most. Boeing states that it is an impractical design because of the amount of mass flow and ducting needed for it to be effective. It was eliminated because of the fact that it was never incorporated into a working aircraft.

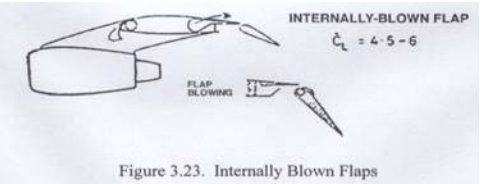

Figure XI.4: Internally Blown Flaps (Ref. 19)

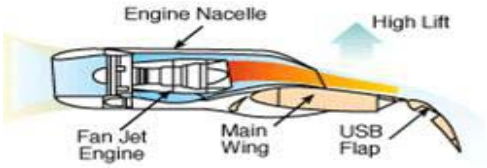

Figure XI.5: Upper Surface Blowing (Ref. 14)

USB, shown in Figure XI.5, was the next best for the lift increment it was capable of developing. While it was incorporated into the design of the YC-14, the An-72/74, the NASA QSRA, and Japan's ASKA, it was deemed too difficult and expensive to develop the proper nozzle configuration. Without a variable area nozzle, it is unable to achieve the optimum conditions for cruise, takeoff, and landing. Therefore whichever condition the nozzle is designed for will cause the others to be highly inefficient. USB also has the undesirable effect of altering the isobars on the upper wing surface during cruise flight. For these reasons, USB was deemed impractical.

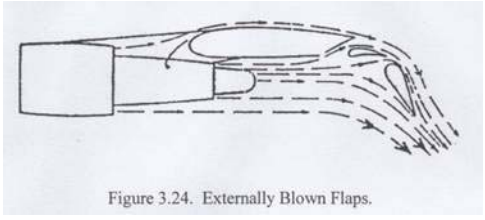

Figure XI.6: Externally Blown Flaps (Ref. 19)

EBF, shown above in Figure XI.6, was the last of the powered lift concepts considered. External blowing significantly increases the lift over traditional slotted flap and slat configurations. The nozzle only needs to be modified such that it assists in spreading the exhaust over as much of the flap as is possible. Less heating problems are encountered since the exhaust is able to mix with the cooler free stream air before meeting the flaps. It is not required to have a unique machine designed for the maintenance of the engines because the engines are located below the wings. This helps to reduce the total cost.

Externally blown flaps were selected for the AAT. EBF takes advantage of powered lift with significantly less design complications than USB or IBF. The US Air Force's C-17 and AMST program were products of similar decisions. The AAT being

proposed has significantly less weight (53,000 lbs vs. 585,000 lbs) and a higher thrust to weight ratio than the C-17 (0.48 vs. 0.28), which allows the AAT to meet the required 2500 ft.

While USB have been used on several test aircraft, they have not been used on any US production aircraft. The Russian An-72 is the only production STOL aircraft in the world using USB (Ref. 12). The YC-15 and C-17 benefited from not having to have a complicated variable nozzle and by having the engines mounted beneath the wing.

2.2. Lift Increment (ΔC_L) Requirements And Comparative Data

An increase in the lift coefficient of as little as one significantly reduces the takeoff thrust needed. Results from various tests and analysis suggest that blown flaps roughly double the maximum lift coefficient, which is useful considering that the takeoff and landing distances stated by the RFP are 40-50% shorter than those achieved by a typical regional jet. A C_L approximately equal to 5.8 will be necessary for takeoff and a C_L of 6.5 will be necessary for landing.

The Boeing 737 achieves a C_{LMax} during landing of 2.7-3.0 using tripled slotted flaps and slats (Ref. 20). Using EBF, a ΔC_L of 2-5 (C_{LMax} = 4.7-8) can be achieved (Ref. 13). The YC-14 and C-17 case studies (Ref. 12, 13) listed the YC-14, YC-15, and C-17 recorded achieving a C_{LMax} in excess of 3.9, 3.4, and 4.2 respectively with double-slotted flaps and some form of powered lift. In an extreme case, the NASA QSRA project attained a C_{LMax} of greater than 10 for a specific configuration. It should be noted that all of the above listed aircraft with the exception of the YC-14, have four engines and therefore have a larger mass flow spread out over a larger flap area than the AAT, which

greatly enhances their maximum lift increment. In addition, only the YC-15 and C-17 used externally blown flaps while the YC-14 and QSRA used upper surface blowing.

All lift increment calculations were based on the determination of the momentum coefficient C_μ. Also known as the blowing coefficient, C_μ is a non-dimensional measure of the mass flow over the blown flaps given by equation 3.

$$C_\mu = \frac{w_j V_j}{gqS} \qquad (3)$$

Using equation 3 and the values from our engines, the C_μ value calculated for the AAT was 2. Equation 4 allowed for a rough approximation of C_{LMax} for the entire aircraft as it includes both the contribution due to engine blowing and the mechanical system's contribution.

$$C_L = (C_L)_{C_\mu=0} + C_\mu \sin(\delta_j + \alpha) + C_{L,\Gamma} \qquad (4)(\text{Ref. } 15)$$

As can be seen in Figure XI.3, the maximum lift coefficient generated by the aircraft with its flap system fully deployed is 4.1, which occurs at an angle of attack (α) of 23 degrees. The pressure lift coefficient was calculated along with the jet deflection angle using Reference 13. This yielded a C_{LMax} for the AAT in excess of 7. From the earlier calculations, it was shown that the maximum C_L needed for takeoff was 5.8 and the maximum needed for landing was 6.5. Because our lift coefficient is so high, the AAT will be able to meet the RFP's BFL requirements.

XII. Stability And Control Surface Sizing:

To initiate the stability study, it was decided that the requirement for stability should be around 10%. This means that the CG at trim should be in front of the neutral point by about 10% of the MAC. Another critical design point was that the aircraft is required to be able to continue the SNI landing with one engine out. The last requirement put forth was that the CG at trim should be in the range of 15-30% of the MAC.

1. Determining The Mean Aerodynamic Chord

MAC is a function of taper ratio and root chord and was found to be 9.9 ft. The location of the MAC both from the LE and from the centerline was found through the use of equations 5 and 6 to be 4.0 ft and 17.3 ft respectively.

$$\bar{x} = \frac{b}{2}\frac{1}{3}\frac{1+2\lambda}{1+\lambda}\tan\Lambda \tag{5}$$

$$\bar{y} = \frac{b}{2}\frac{1+2\lambda}{3(1+\lambda)} \tag{6}$$

2. Initial Tail Sizing

The first values needed to size the tail were the vertical and horizontal volume coefficients. Using a primarily historical method, the values of V_V and V_H were found to be 0.065 and 1.3 respectively

$$S_H = \frac{V_H S_W \bar{c}_W}{l_H} \tag{7}$$

$$S_V = \frac{V_V b S_W}{l_V} \tag{8}$$

Through the use of equations 7 and 8, Figure XII.1 was developed. This plot illustrates the effect that the vertical and horizontal moment arms have on the area needed for the tail surfaces.

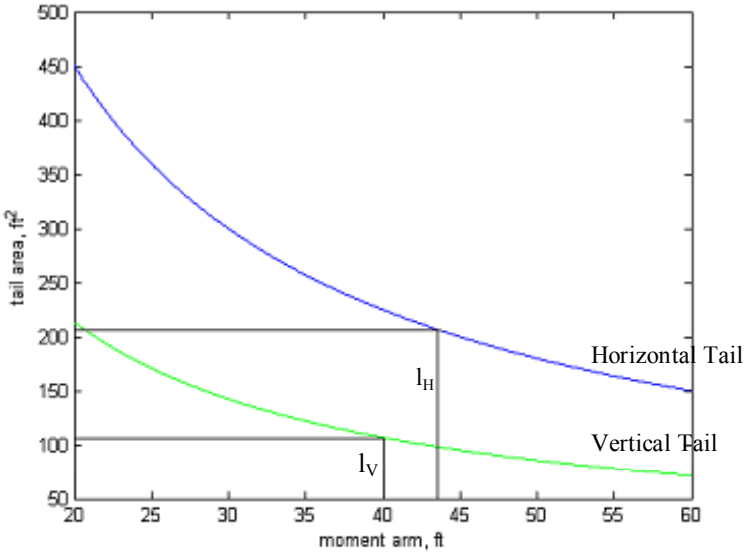

Figure XII.1: Constraining Equations For Horizontal And Vertical Tail Areas

The vertical and horizontal lines on the plot represent the chosen moment arms and their correlating areas of 106.9 ft^2 for the vertical surface and 205.7 ft^2 for the horizontal surface. By using typical geometry formulas, the following numbers were calculated.

Table XII.1: Resulting Sizes Of Vertical And Horizontal Surfaces

	Vertical	**Horizontal**	**Units**
S	106.9	205.7	ft^2
c_{bar}	10.34	6.7614	ft
b	10.34	30.43	ft
AR	1.0	4.50	
Λ	20.00	20.00	deg
λ	0.88	0.5025	
c_r	11.0	9.0	ft
c_t	9.68	4.52	ft

3. Longitudinal Control

Using the above numbers for the horizontal tail as a starting point and a vortex lattice method program called JKayVLM (Ref. 18), the horizontal stability derivatives were derived and the AAT's overall horizontal stability was measured. After running the program with an elevator of 0.25c, it was found that the tail did not need any resizing because it was at the desired stability. The AAT was designed to be 10.2% stable at trim. Using the derivatives shown in Table XIII.2 and the CG at trim, the neutral point and CG range were calculated. The neutral point was calculated to be 30.3% MAC and the range was found to be from 15.9-30.3% MAC with the aft limit being at the neutral point.

Table XII.2: Horizontal Derivatives

Horizontal Derivative	Value
$C_{L\delta a}$	-4.733
$C_{m\delta a}$	0.0299
C_{L0}	0.114
C_{m0}	-0.00315
C_m/C_L	-0.1016

4. Lateral Control

By using the dimensions listed above for the vertical tail as a starting point, a program called LDstab (Ref. 18) was used to find the vertical stability derivatives and the finalize the size of the vertical surface. The program was run using a rudder of 0.25c and it was found that the vertical tail was not large enough to compensate for engine out conditions. This led to the vertical tail being increased until it was the dimensions shown in Table XIII.3. This allowed the tail to be able to counter the large moments involved in the engine out condition.

Table XII.3: Final Sizing Values From Engine Out Conditions

	Vertical	**Units**
S	235.3	Ft^2
c_{bar}	15.34	Ft
b	15.34	Ft
c_r	16.0	Ft
c_t	14.70	Ft

5. Roll Control

Due to the need for high lift, it was decided that a combination aileron-flap system (flaperon) would be used. This meant that the ailerons had to be 28% of the wing's local chord to match that of the flap system and to allow for it to be anchored to the rear spar of the wing. By using a method found in Reference 1, each flaperon was found to have semi-span of 17.1 ft measured from the wing tip in order to provide sufficient roll control. Unfortunately, only 10 ft per semi-span was allowed for the flaperons due to the complicated mechanical flap system for high lift. To compensate for this, a roll control spoiler will be used.

XIII. Structures:

1. Material Selection

The five factors considered in the selection of a material for a particular component were: cost, strength to weight ratio, familiarity, experience, and corrosion resistance. One of the largest factors in any design is always the weight. It was decided that, in order to save weight, the AAT use composite materials in non-critical areas. The materials used are illustrated in Figure XIII.1.

1.1 Fuselage

An aluminum alloy is typically used as both the skin and the framework for the fuselage of many commercial airplanes. The main reasons for this are that aluminum can sustain greater bending loads than steel can and that it is corrosion resistant. As an alternative to the standard aluminum, a new skin technology called GLARE was considered also. GLARE is a material consisting of alternating layers of aluminum and fiberglass. This system of alternating layers would allow for a higher strength to weight ratio than pure aluminum. However, because of the lack of sufficient data proving its reliability, it was quickly eliminated. The final material chosen for the skin was an aluminum alloy designated 2024-T3 while 7075-T6 aluminum alloy was chose for the frame.

1.2 Wing

For the spar, skin, and stringers, 7075-T6 aluminum was chosen while for the ribs and slats, it was determined that 2024-T3 aluminum would be used.

In an effort to save as much weight as possible, it was decided that much of the flap system would be made from composites. Because carbon fiber-reinforced polymers are relatively inexpensive and have the highest specific modulus and specific strength of all reinforcing fiber materials they were chosen for use on the flaps and ailerons. However, because hot exhaust gases from the engines had to be taken into account for blown sections of the flaps it was determined that the use of a Titanium alloy would be better because of its high melting point of 3035°F. For engine mounts, Aramid fiber-reinforced polymer composite known as Kevlar were chosen because they are resistant to combustion and stable to relatively high temperatures.

1.3 Empennage

It was decided that the materials used in the wing were sufficiently strong enough to be used for the empennage. For the vertical and horizontal tail skins, stringers, and spars, 7075-T6 aluminum was chosen and 2024-T3 for the ribs. To save more weight, carbon fiber-reinforced polymer composites would be used on the elevator and rudder.

1.4 Landing Gear

Intense cyclic loads had to be considered for the landing gear struts and the structural joints, therefore steel was selected for its high durability.

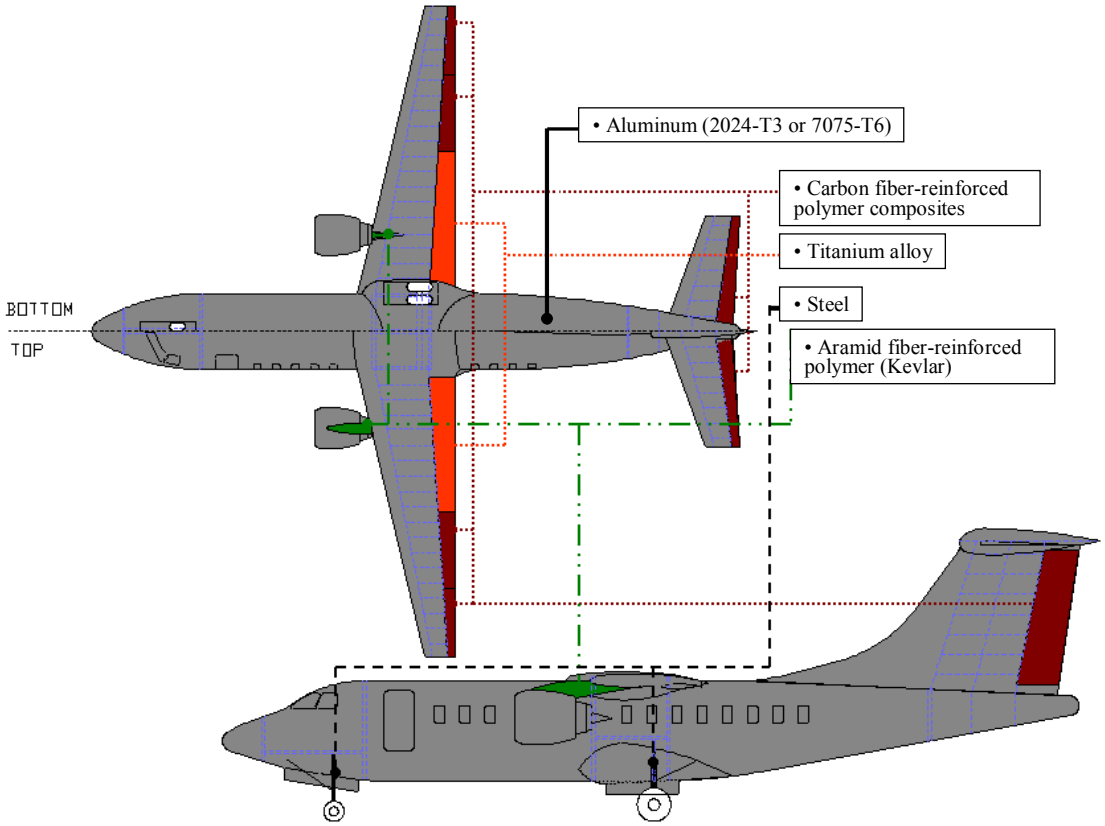

Figure XIII.1: Material Locations

2. Structural Layout

As with most aircraft, the structural layout of the AAT consists of frames, bulkheads, longerons, ribs, and spars. The arrangement of this structural layout is based on typical structural spacing and arrangements presented in Reference 5 and are illustrated in Figure XIII.2.

2.1 Fuselage

For the fuselage, the frame spacing was set at 20 in with a depth of 1.5 in. The longerons have a spacing of 10 in. Bulkheads are always located at high load areas to increase the strength. These areas include the front and rear pressure bulkheads, nose and main landing gear bulkheads, wing spar bulkheads, and horizontal tail spar bulkheads.

2.2 Wing And Empennage

Both the wing and the tail surfaces have their main spars located at 25%c. Because the rear spars will act as hinge points for the control surfaces and the flap system, the size of the surface drives their position. For the wing, the rear spar is located at 72%c while for empennage the rear spars are located at 75%c. Rib spacing for the wing and empennage section is 24 in.

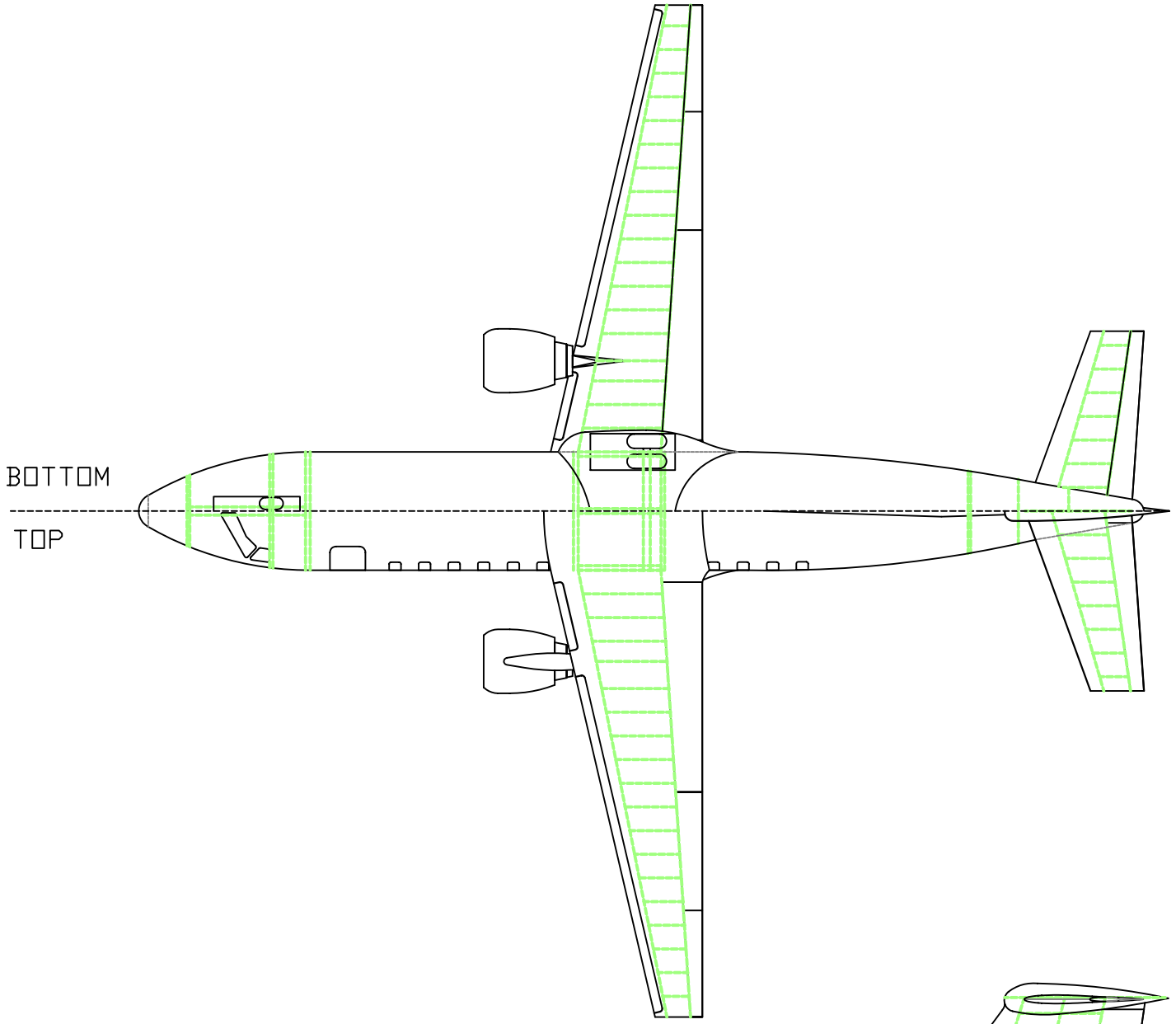

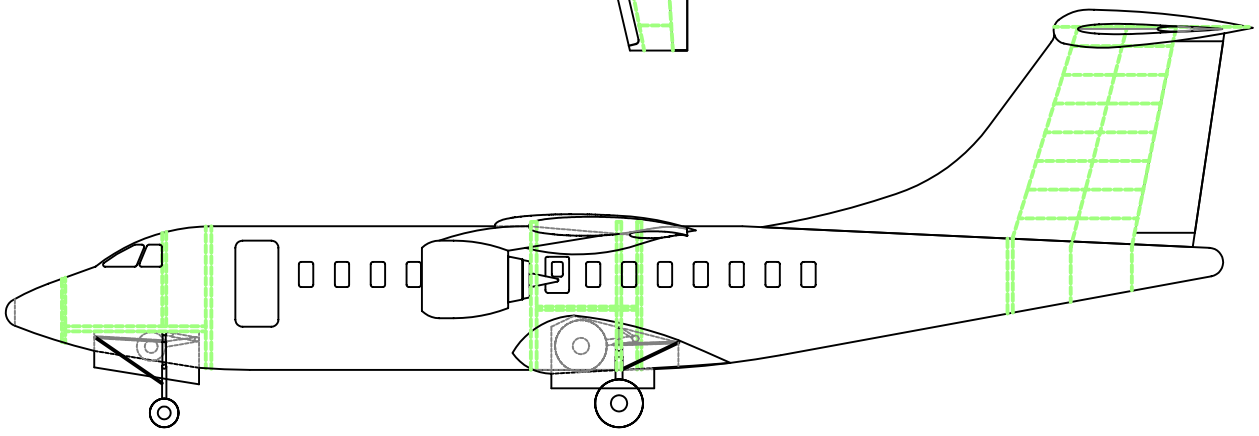

SCALE (FT)

0 10 20 30 40

WING RIB SPACING = 24 IN.
FUSELAGE FRAME SPACING = 20 IN.
FUSELAGE LONGERON SPACING = 10 IN.

TEAM BACCHUS	
STRUCTURE OVERVIEW	AIRCRAFT MODEL: AAT-100
	DRAWING VERSION: 2.7
	REVISON DATE: 5/2/2004 M.T.

3. Load Requirements And Fulfillment

The V-n diagrams shown in Figure XIII.3 and Figure XIII.4 summarize the load requirements and load factors for symmetrical maneuvers listed in the FAR 25.337(b),(c) and the FAR 25.345(a)(1),(b). For positive maneuvers up to the dive speed (V_D), the load factor is 2.5. For negative maneuvers up to cruise speed (V_C), the load factor is –1. From cruise speed to dive speed; the load factor varies linearly from -1 to 0. The FAR 25.341(a) specifies load factors of a flight in turbulence. The table shown below, Table XIII.1, is a summary of the gust velocities in the three conditions. For example, for the stall boundary speed (V_B), gust velocity is 66 ft/sec from sea level to altitude of 20,000 ft. However, the gust velocity varies linearly from 66 ft/sec to 38 ft/sec at altitude from 20,000 ft to 50,000 ft.

Table XIII.1: Summary Of The Gust Velocities In The FAR 25 (Ref.6)

	0 to 20,000 ft	50,000 ft
V_B	66 ft/sec	38 ft/sec
V_C	50 ft/sec	25 ft/sec
V_D	25 ft/sec	12.5 ft/sec

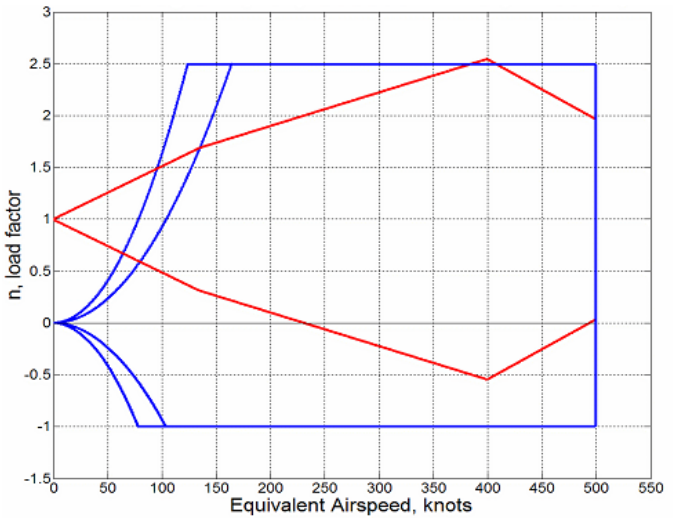

Figure XIII.3: V-n Diagram For Fully Loaded Primary Mission

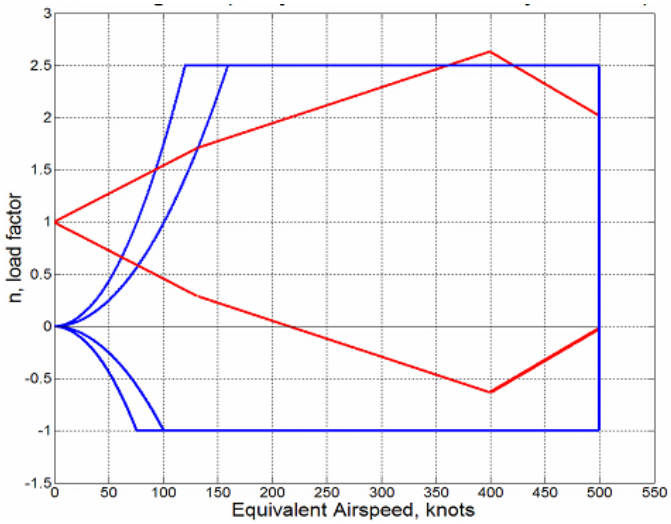

Figure XIII.4: V-n Diagram For Fully Loaded Secondary Mission

4. Landing Gear Design

The landing gear for the AAT was designed based on nose gear steering loads and landing load presented in the FAR 25. To maintain adequate steering control, it is specified in Reference 7 that the nose gear must carry at least 8% of the TOGW. Therefore, the location of the nose gear was chosen 132.5 in from the nose, while the main gear was located 512.4 in from the nose. The nose gear was designed to be able to withstand 9% of the TOGW.

The touchdown rate specified in FAR 15.723 was 12 ft/sec and was the critical factor in designing the landing gear. Both the nose and main landing gears are strut-braced, dual wheel systems that have oleo-pneumatic shock absorber. Each main gear has a stroke of 17 in and the nose gear has a stroke of 11 in. Both gears retract forward, allowing for free-fall capability in the event of a failure in the extension system, see Figure XIII.5. Retractional kinematics was determined based on a method presented in Reference 8.

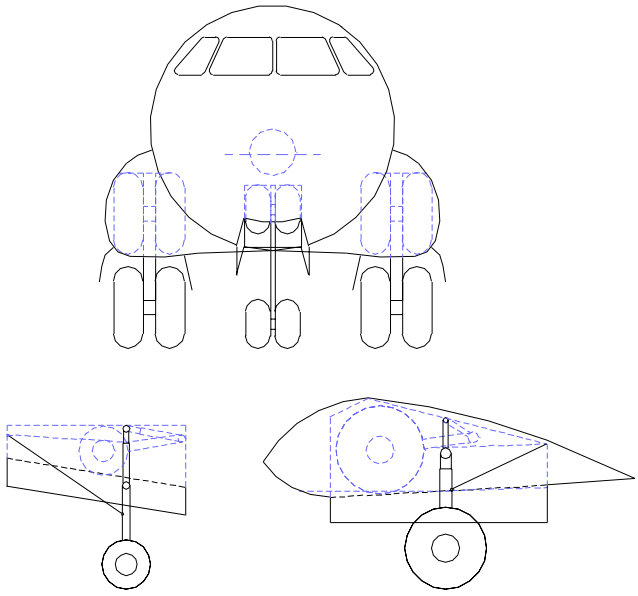

Figure XIII.5: Landing Gear Retraction System

Type VII tires were chosen for the main and nose gear. For the primary mission, each tire on main gear has an outer diameter of 36 in and a width of 11 in, while each tire on nose gear has an outer diameter of 24 in and a width of 5.5 in. For the secondary mission a bigger tire was chosen for the main gear because of the provision made for semi-prepared landing zones in the RFP. They were chosen to have an outer diameter of 40 in and a width of 14 in. The size of the nose gear stayed the same for both missions.

XIV. Systems:

Because of the nature of the AAT, there are certain specifications that go above and beyond what would normally be considered. While the AAT must follow all the requirements normally set forth in the development of an RJ, the RFP requires the additional features or operations:

- The AAT must be able to conduct a SNI Adverse Weather Approach.
- It must be able to perform an automated spiral descending decelerating approach in IMC (CAT 3C) conditions.
- It must be able to continue the approach with one engine inoperative.

1. Cockpit Design

Although the general layouts of the instruments are similar to conventional regional jets, several additional features were considered in order to better suit this aircraft. Firstly, instead of using flight yoke, a joystick style control was selected because of its greater range of motion. The control stick was located at the tip of the outer armrest, which allows the pilot to better access to the control panel. Secondly, because the AAT is required to perform landings at high angles of attack in all weather conditions, a Heads-Up-Display (HUD) will be of a great aid to the pilot. Lastly, a set of Multi-Function Displays (MFD) will be included on the control panel to control and display the digital systems. Other key components that are standard to most our comparator aircraft and that will be included in the AAT are:

- Thrust management system
- Engine failure detection system

- Radio communication equipment
- Autopilot/Flight director
- Analog instrument backups: altimeter, airspeed indicators, attitude indicators, gyroscopic and magnetic compass, turn-slip / bank indicator
- MFD: meteorological reporting, digital altitude/attitude indicator, digital compass
- Flight data recorder/ Voice recorder

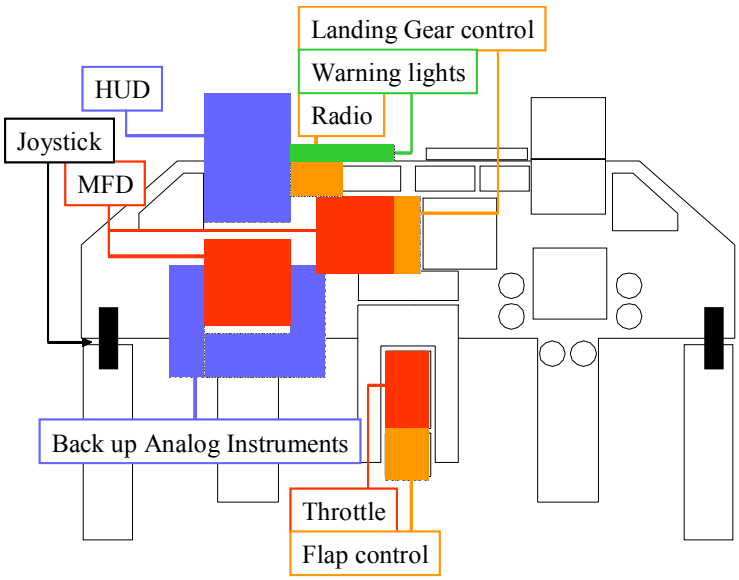

Figure XIV.1: Cockpit Control Panel

2. Flight Control Systems (FCS)

Due to its difficult nature of thrust control in case of emergency (loss of an engine) a Fly-By-Cable system cannot be applied because of its response time; therefore either a Fly-By-Light or a Fly-By-Wire system was needed. Because of the similar nature of the two systems, cost was the deciding factor between the two. The Fly-By-Light system cost more than the Fly-By-Wire system while both had an acceptable response time.

A digital Stability and Control Augmentation System (SCAS) was added to augment the natural stability of the AAT. This system aids the pilot during all phases of flight, but is most beneficial during high angle of attack flight and engine out conditions. The SCAS for the AAT will be integrated with the autopilot systems to make the plane easier to fly and decrease the pilot workload.

A Thrust Management System (TMS) and an Engine Failure Detection System (EFDS) were added in addition to the aforementioned SCAS to aid the pilot in the event of an engine out situation. Minimizing the detection and reaction time is critical in the event of an engine failure during the takeoff and landing phases of flight. TMS, EFDS, and SCAS working together reduce the time between the detection of an engine failure and the time it takes to respond appropriately with the controls. These systems are designed to detect an engine failure before the pilot even knows what has happened and to automatically reconfigure the flight controls to counter the loss of lift and yawing / rolling due to the engine failure when the EBF system is in use. This will improve the overall safety and limit the altitude and control loss.

3. Hydraulic system

The control surfaces of this aircraft are controlled using hydro-electrostatic actuators. These actuators combine electric and hydraulic power to effectively move control surfaces. The actuators attain their power through the use of engine-driven generators and pumps. The actuators are also utilized to raise and lower the landing gear.

4. Electric system

During flights, the equipped systems will be operated by power supplied from two engine-driven generators. The Auxiliary Power Unit (APU) will provide the power to operate the systems and to start the engine while the aircraft is on the ground. The third device used is the Ni-Ca battery. Its purpose is to provide initial power to the APU as well as the core systems in case of emergency. This battery will only last for a short while. The power systems are shown below in Figure XIV.2.

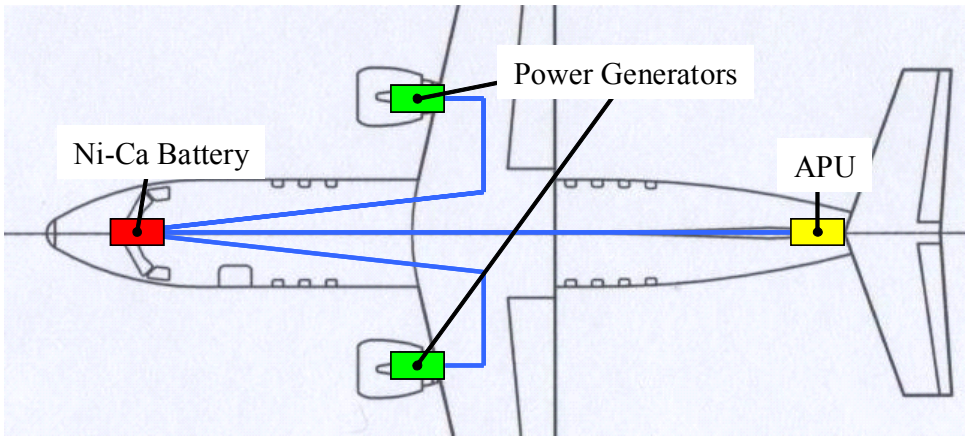

Figure XIV.2: Diagram Of Power Subsystems

5. Fuel system

To store the bulk of the fuel there are three separate compartments located in the wing. They are capable of storing 229 ft^3 of fuel and are illustrated in Figure XIV.3 below. The main tanks are located on the inboard portions of the wing while the reserves are located in the outboard tanks. This helps to reduce both the amount of piping and the amount of shift in the CG during flight.

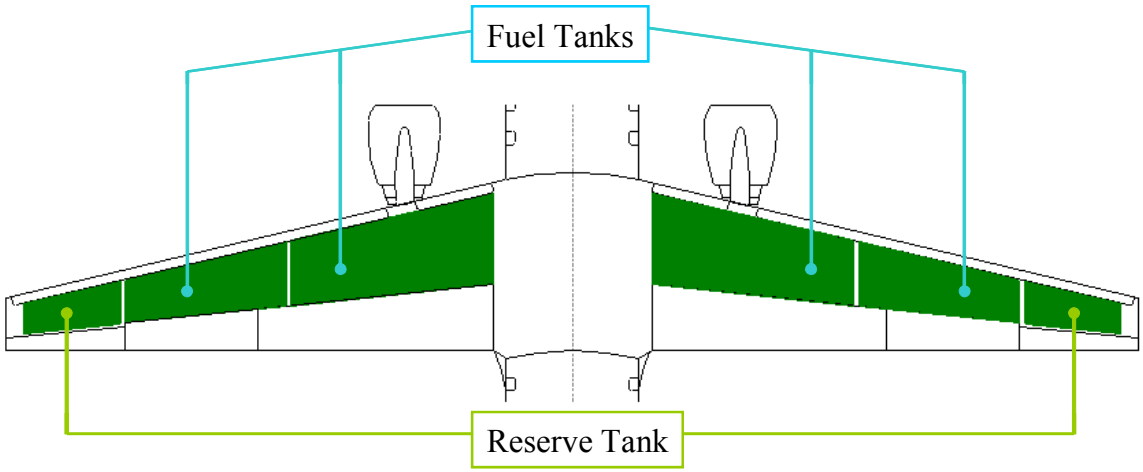

Figure XIV.3: Fuel Tank Diagram

6. De-Icing system

The de-icing system for this aircraft consists of a series of low cost and light weight thermoelectric heating devices located along the leading edge of the wing. Although it is simple mechanism, it is effective and only requires electricity to be activated.

7. Oxygen System

The oxygen system for the AAT is composed of two individual systems; a cockpit system and cabin system. To ensure safety, the cockpit oxygen system was designed to have priority over the cabin oxygen system. Oxygen masks for use in the cabin are stored in the overhead compartments, and will be deployed in event of a sudden pressure drop. Portable oxygen tanks are available for the use of cabin crew.

XV. Cost Estimation And Subsidization:

Current trends in airport usage indicate that more traffic can be expected in the future. With the incorporation of STOL technologies, the AAT has the solution to this problem. With this capability, the AAT has an advantage over comparator aircraft in the sales to international countries that have limited airport area. As was previously stated, the AAT is also capable of acting as a troop transport. This would be particularly important to countries located around fault lines where the potential for earthquakes in residential areas is high. With the additional capabilities and benefits of the AAT, this aircraft is a clear choice for purchase.

Not only does the AAT meet all RFP requirements, but it is also cost effective to both the government and the airline company. In order to keep the cost of the aircraft down, an early decision was made to include only those technologies that had been proven on other aircraft and to simplify the modification process by only including the required extra systems. With this being said, the amount of government subsidization was the driver for deciding on the amount of extra systems, which would be included on the AAT/WFS aircraft. Currently, the amount of subsidization required by the government is only three to seven million dollars per aircraft and was based on comparator aircraft cost. The AAT/WFS aircraft cost is approximately three million more than the ERJ 145 and seven million more than the CRJ 200. If the government decides to increase the amount of money available, the design of the AAT/WFS aircraft could therefore increase the amount of available systems to improve its mission capabilities.

The empirical formulas, described by Reference 4, were used to estimate the cost for the AAT program. Because *Roskam's* cost estimation technique is based on the historical statistical data of various airplane programs, the results of the cost analysis is a rough estimation of the true cost of the AAT program. All the statistical coefficients of the equations were modified to current conditions prior to analysis by making reasonable assumptions based on the depreciation periods of airplanes. The cost estimation analysis of the AAT program consists of six major phases: Phase 1: Planning and Conceptual Design, Phase 2: Preliminary Design and System Integration, Phase 3: Detail Design and Development, Phase 4: Manufacturing and Acquisition Cost, Phase 5: Operation and Support, and Phase 6: Disposal. The remainder of this section will be devoted to these topics.

1. Phase 1-3: Research Development Test And Evaluation (RDT&E) Cost (C_{RDTE})

These are the costs for the research, development, conceptual and detailed design drawings as well as for the associated financing and profit. The costs for these phases were estimated using a total of 5 RDT&E aircraft. Three of the aircraft were to be used as prototypes and two for dynamic and static structural testing. Calculations for both primary and secondary versions were done simultaneously due to the similar airframe configurations, engines, and avionics systems.

The six factors that were used to develop the RDT&E costs were: technology difficulty factor, TOGW, empty weight, maximum design speed, avionics, and engine costs. The avionics systems were estimated to cost $2.1 million. Two CF34-8C1 engines were estimated to cost $5 million. Table XV.1 and Figure XV.1 below show the cost and

percentage breakdown for the RDT&E phases based on the current value of the US dollars. The final cost of the RDT&E phase was estimated to be 771 million dollars. This total RDT&E cost is twice as high as that of the current ERJ 145 program since the AAT was deemed to have a high technology difficulty factor due to the additional mission capability. This is the main factor of the cost inflation.

Table XV.1: Cost Break Down For RDT&E Phase

Phase 1 – 3	**Cost***
Airframe Engineering & Design Cost	$116.9
Development Support & Test Cost	$ 38.9
Flight Test Airplanes Cost	$420.2
Flight Test Operational Cost (OC)	$ 10.2
Test & Simulation Facilities Cost	$ 30.9
Profit For RDT&E Phase	$ 77.1
Cost To Finance Of The RDT&E phase	$ 77.1
TOTAL	**$771.3**

*In Millions Of US Dollars

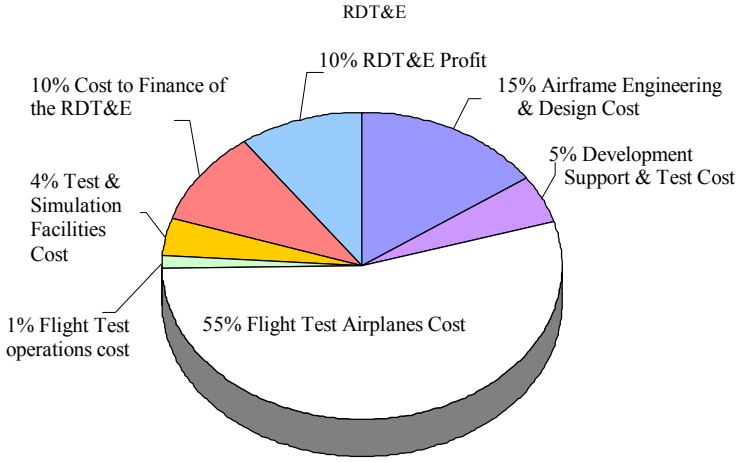

Figure XV.1: Percentage Breakdown For RDT&E Phase

2. Phase 4: Manufacturing And Acquisition Cost (C_{MAN}, C_{ACQ})

These costs are necessary for the manufacturing, production, flight-testing, profit, and financing for the entire airplane through the program, excluding RDT&E phase

airplanes. The costs are determined using the aircraft's weight, maximum design speed, technology factors, and the cost of the avionics systems and engines. They were estimated using a production run of 500 airplanes. Table XV.2 below shows the cost breakdown for this phase. The final cost for phase 4 was estimated to be 9,294 million dollars for the primary mission.

Table XV.2: Manufacturing And Acquisition Costs Breakdown

Phase 4 (500 airplanes each)	
Mission Statement	**Primary Mission**
	Cost*
Airframe Engineering & Design Cost	$ 155.1
Airplane Production Cost	$7,413.4
Production Flight Test OC	$ 36.0
Cost To Finance Manufacturing Program	$ 844.9
Total C_{MAN}	$8,449.4
Profit For Manufacture Program	$ 844.9
Total C_{ACQ}	$9,294.4
TOTAL - C_{ACQ}	**$9,294.4**

*In Millions Of US Dollars

3. Phase 5: Operational And Support Cost (C_{OPS})

The OC's, shown in Table XV.3, are the summation of the fuel, direct and indirect personnel, consumable materials, spare parts, and depot, finance to the operational program, and indirect operational cost (IOC). Since the IOC is difficult to approximate, Roskam suggests estimating the IOC to be 50% of the direct operational cost (DOC). OC's were estimated for production runs of 150, 500, and 1500 airplanes for each mission. The active service for the airplanes was assumed to be 20 years.

Table XV.3: Operational Cost Breakdown

Phase 5	**Active service 20 years assumed**					
	150 airplanes		**500 airplanes**		**1500 airplanes**	
Mission Statement	**PM**	**SM**	**PM**	**SM**	**PM**	**SM**
	Cost* ($/nm)					
Flight OC	3.400	2.880	3.126	2.697	2.998	2.612
Maintenance Cost	3.444	3.298	3.094	2.973	2.931	2.822
Depreciation Cost	2.935	1.578	2.289	1.238	1.988	1.079
Depot	0.081	0.071	0.079	0.069	0.078	0.069
Finance to Operation Program	0.742	0.589	0.646	0.525	0.602	0.495
Total DOC	10.602	8.416	9.234	7.503	8.597	7.078
Total IOC	5.301	4.208	4.617	3.751	4.298	3.539
Total OC	**15.903**	**12.624**	**13.851**	**11.254**	**12.89**	**10.617**
	Cost* ($)					
Total DOC	35.24	50.92	102.30	151.34	285.70	428.30
Total IOC	17.62	25.46	51.12	75.67	142.87	214.15
Total C_{OPS}	**52.86**	**76.39**	**153.45**	**227.00**	**428.59**	**642.45**

*In Billions Of US Dollars

OC's are highly dependent on the ratio of aircraft produced for the primary and secondary missions and the frequency for which the aircraft are used for the secondary mission. The results of the table are based on the maximum usage of each primary and secondary airplane. The total C_{OPS} of the primary mission are higher than that of the secondary mission due to the differences in the block ranges and flight time.

4. Phase 6: Disposal Cost (C_{DISP})

The disposal cost is defined as 1 percent of the total life cycle cost. The total disposal cost was estimated to be $1,650 - $2,390 million for the current value of the US dollars for production runs of 500 airplanes.

5. Life Cycle Cost (LCC)

Production runs of 500 airplanes were used when determining the LCC and unit costs at each phase. Excluded from those costs are the five RDT&E airplanes. The unit cost for the manufacturing, acquisition, and estimated airplane life cycle are shown in Table XV.4.

Table XV.4: Unit And Life Cycle Cost

Unit Cost, 500 Airplanes Each	**For Active Service 20 Years**
Mission Statement	**Primary**
	Cost*
Manufacture unit Cost, C_{MAN}/NM	16.9
Acquisition unit Cost, C_{ACQ}/NM	18.6
Estimated Airplane Cost-AEP	20.1
Life Cycle Unit Cost	330.3
LCC	165,100

*In Millions Of US Dollars

Using *Roskam's* technique, the estimated airplane cost (AEP) is usually $2~3 million less than the market price of the airplanes. The differential amount will be added to determine the actual airplane cost of the plane.

6. Fly Away And Operational Cost

Cost estimates for each phase were based on the production of all airplanes being of the same type or mission. In general, the AAT program is a combination of primary

and secondary missions. The number of airplanes produced for each mission will be dependent on the demand by each airline and the quantity of dual-use aircraft desired. The fly away cost and OC's were estimated assuming that significantly more aircraft will be produced solely for the primary mission vs. those capable of supporting the secondary mission requirements. Table XV.5 shows the fly away cost and OC assuming that 10% of the aircraft produced for an airline are to be used for the secondary mission. A trend to notice is that the cost for all phases decreases dramatically as the number of airplanes increases. As the primary and secondary aircraft share much in common, the cost differential is due to the interior changes resulting from the mission requirements and the need to carry the additional fire suppressant Figure XV.5 shows a trend of this cost analysis that the cost per one airplane for all phases decreases dramatically as the number of airplanes increases.

Table XV.5: Fly Away And Operational Cost

	Assumed Active Service For 20 Years					
	150 Airplanes		**500 Airplanes**		**1500 Airplanes**	
Mission Statement	**PM**	**SM**	**PM**	**SM**	**PM**	**SM**
Number Of Aircraft	135	15	450	50	1350	150
	Cost* ($)					
Manufacture Unit Cost - C_{MAN}/nm	22.4	37.1	17.3	26.5	14.2	21.2
Acquisition Unit Cost - C_{ACQ}/nm	24.6	40.8	18.9	33.2	15.7	23.4
Fly Away Cost	19.3	31.2	15.1	23.6	12.6	18.4
Total Fly Away Cost	20.49		15.95		13.18	
	Cost* ($/nm)					
Total DOC	10.78	14.94	9.318	7.503	8,643	8.416
Total IOC	5.392	7.468	4.659	3.751	4.322	4.208
OC = DOC + IOC	16.171	22.408	13.977	11.254	12.965	12.624
Total OC	**16.794**		**13.705**		**12.931**	
OC/hr	**$/hr 5663.3**		**$/hr 4753.9**		**$/hr 4355.5**	

*In Millions Of US Dollars

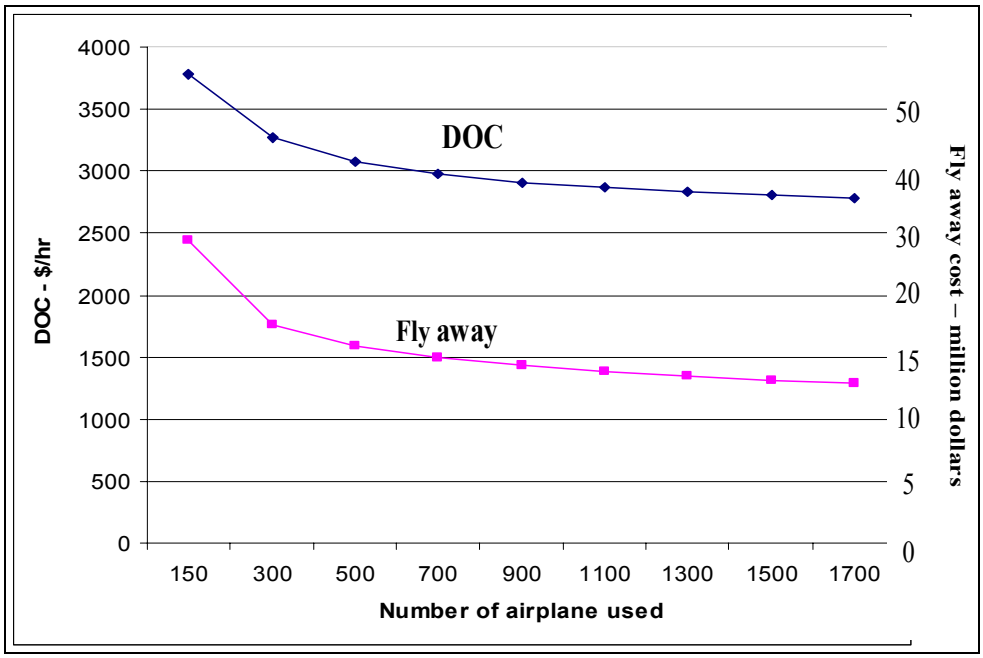

Figure XV.5: Fly Away And Direct Operational Cost

From Figure XV.5, without government subsidization, the AAT needs to produce more than 1700 airplanes in order to achieve the price of either comparator RJ (ERJ145 or CRJ200).

7. Summary Of The Cost Analysis

Table XV.6 shows the final summary of the cost analysis. As can be seen, the OC of the AAT is higher than the comparator RJ's because it accounts for 10% of the aircraft to be used for the secondary mission. If the secondary mission is not carried out, about 200 dollars per block hour will be saved from the total OC. Although the market price of the aircraft varies from 17.5 to 28.1 million US dollars, the unit price per aircraft is very competitive with current comparator RJ's when the amount of the government subsidization is taken into account.

Table XV.6: Operating And Unit Cost Comparison

Operating Cost/Unit Cost Comparison		
Assumed 1650 nm trip for each aircraft (1500 nm mission + 150 nm diversion)		
TYPE	**DOC+ICO $/hr**	**Airplane Market Price (Millions Of US Dollars)**
AAT-100		
(150 aircrafts)	5663	28.1
(500 aircrafts)	4616	21.9
(1500 aircrafts)	4360	17.5
CRJ 200	3840	20.1
ERJ 145	3680	15.1

XVI. Conclusion:

The AAT combines the perfect blend of STOL technologies and cost effectiveness through the use of proven technologies. With its capability of using short runways, it is ideal for the airline company who is not only trying to branch out to smaller airports, but also one who values customer service. Customer service will increase because the low cost of the AAT will be reflected in lower ticket prices than competitor aircraft. All this and the AAT still ranks in the same cost bracket if not lower than its competition.

If an airline company chooses to have the AAT equipped to serve in the Civil Reserve Fleet, it could play a crucial role in saving land, homes, or even lives. With the government's offer to subsidize the airline company, these benefits come at only a minor time inconvenience. If the government chooses to increase the amount of subsidization the flexibility of the AAT would dictate that it could be outfitted to perform a variety of extra missions.

This being said, Team Bacchus is confident that the superior design of the AAT will yield a large return and is an excellent investment for any airline company wishing to save money.

References

1. AIAA. 2003/2004 AIAA Foundation Undergraduate Team Aircraft Design Competition. Sep. 2003. American Institute of Aeronautics and Astronautics. <http://www.aiaa.org/education/students/2003-2004UgradAircraft.doc>.

2. Raymer, D. P., *Aircraft Design: A Conceptual Approach*, 3rd ed., AIAA, Virginia, 1999

3. Roskam, J., *Airplane Design; Part VI: Preliminary Calculation of Aerodynamic, Thrust and Power Characteristics*, DARcorporation, Kansas, 2000

4. Roskam, J., *Airplane Design; Part VIII: Airplane Cost Estimation: Design, Development, Manufacturing, and Operating*, Roskam Aviation and Engineering Corporation, 1990

5. Roskam, J., *Airplane Design; Part III: Layout Design Of The Cockpit, Fuselage, Wing And Empennage: Cutaways And Inboard Profiles*, Roskam Aviation and Engineering Corporation, Kansas, 1989-91

6. Lomax, T., *Structural Loads Anaylsis For Commercial Transport Aircraft: Theory And Practice*, AIAA, Virginia, 1996

7. Roskam, J., *Airplane Design; Part IV: Layout Design Of Landing Gear And Systems*, Roskam Aviation and Engineering Corporation, Kansas, 1989-91

8. Curry, N., *Aircraft Landing Gear Design: Principals And Practices*, AIAA, Washington D.C., 1988

9. Bill, Obe, Fraes, Gunston, *Jane's Aero Engines*, Jane's Information Group, New York, 1996

10. Abbott and Von Doenhoff, *Theory of Wing Sections Including A Summary Of Airfoil Data*, Dover Publications Inc., New York, 1959

11. McCormick, B. W., *Aerodynamic Astronautics And Flight Mechanics*, 2nd ed., John Wiley & Sons Inc, New York, 1995

12. Norton, B., *STOL Progenitors: The Technology Path To A Large STOL Aircraft And The C-17A*, AIAA, Virginia, 2002

13. Wimpress and Newberry, *The YC-14 STOL Prototype: Its Design, Development, and Flight Test*, AIAA, Virginia, 1998

14. ASKA. ASKA. Sep. 2003. Japan Aerospace Exploration Agency <http://www.nal.go.jp/flight/eng/Museum/ASKA/aska.html>.

15. Davenport, E. E., *Wind-Tunnel Investigation Of External-Flow Jet-Augmented Double Slotted Flaps On A Rectangular Wing At An Angle Of Attack Of 0° To High Momentum Coefficients*, NACA, Washington D.C., 1957

16. GE Transportation Aircraft Engines. The CF34 Engine Family. Oct. 2003. <http://www.geae.com/engines/commercial/cf34/index.html>. General Electric. <http://www.ge.com/en >.

17. CFM International. CFM56 Engine Family. Oct. 2003. <www.cfm56.com>.

18. Mason, Crisafulli. AOE 4065-4066 Design (Aircraft). 2003, 2004. <http://www.aoe.vt.edu/~mason/Mason_f/ACDesSR/content.html>. Virginia Tech Department of Aerospace and Ocean Engineering. <www.aoe.vt.edu>.

19. Marchman III, J. F., *Introductory Aircraft Performance*, 2nd ed., A-1 Copies, Virginia, 2001

20. Brady, Chris. History & Development of the Boeing 737. Nov. 2003. <www.b737.org.uk/history.htm>.